의학박사 학위논문

The effect of solute carrier organic transporter family member 2B1 genotype and cytochrome P450 3A activity on the pharmacokinetic characteristics of voriconazole

Solute carrier organic transporter family member 2B1 유전형 및 CYP3A 대사능이 voriconazole 의 약동학적 특성에 미치는 영향 평가 연구

2020 년 08 월

서울대학교 의과대학 대학원

협동과정 임상약리학전공

이 상 원

A thesis of the Degree of Doctor of Philosophy

Solute carrier organic transporter family member 2B1 유전형 및 CYP3A 대사능이 voriconazole 의 약동학적 특성에 미치는 영향 평가 연구

The effect of solute carrier organic transporter family member 2B1 genotype and cytochrome P450 3A activity on the pharmacokinetic characteristics of voriconazole

August 2020

Department of Clinical Pharmacology and Therapeutics, Seoul National University College of Medicine
Sang Won Lee

Solute carrier organic transporter family member 2B1 유전형 및 CYP3A 대사능이 voriconazole의 약동학적 특성에 미치는 영향 평가 연구

지도 교수 정 재 용

이 논문을 의학박사 학위논문으로 제출함
2020년 8월

서울대학교 대학원
협동과정 임상약리학전공
이 상 원

이상원의 의학박사 학위논문을 인준함

2020년 8월

위 원 장 장 우 경 (인)
부위원장 정 재 용 (인)
위 원 박 완 범 (인)
위 원 김 홍 빈 (인)
위 원 김 정 렬 (인)

The effect of solute carrier organic transporter family member 2B1 genotype and cytochrome P450 3A activity on the pharmacokinetic characteristics of voriconazole

by
Sang Won Lee

A thesis submitted to the Department of Clinical Pharmacology and Therapeutics in partial fulfillment of the requirements for the Degree of Doctor of Philosophy in Medicine at Seoul National University College of Medicine

August 2020

Approved by Thesis Committee:

Professor Chijin Jang Chairman
Professor Jae Yong Chung Vice chairman
Professor Wan Beom Park
Professor Hong Bin Kim
Professor Jungryul Kim

ABSTRACT

Introduction: High pharmacokinetic variability of voriconazole is mainly explained by CYP2C19 phenotype, but there are still unknown factors affecting the variability.

Methods: In this study, the effect of solute carrier organic anion transporter family member 2B1 (SLCO2B1) genotype on the pharmacokinetics (PKs) of voriconazole was evaluated in 12 healthy CYP2C19 poor metabolizers after a single administration of voriconazole 200 mg intravenously and orally. A model-based simulation was done to further explore the effect of SLCO2B1 genotype on the pharmacokinetics of voriconazole. In addition, the influence of CYP3A4 enzyme activity was also explored.

Results: The oral absorption of voriconazole was decreased and delayed in the subjects with the SLCO2B1 c.*396T>C variant compared to the subjects with wild-type. However, the CYP3A activity markers measured in this study did not show significant association with metabolism of voriconazole. SLCO2B1 genotype did not seem to have a significant effect on the probability of reaching therapeutic range after a standard voriconazole dosing regimen.

Conclusions: The results suggest that the SLCO2B1 c.*396T>C

may be associated with the decreased function of intestinal OATP2B1, and it could contribute to inter-individual PK variability of voriconazole. The clinical relevance of these findings should be confirmed through further investigations.

* Part of this work has been published in *the Pharmacogenomics Journal.* (LEE, Sang Won, et al. *The Pharmacogenomics Journal*, 2020, 1-9; https://doi.org/10.1038/s41397-020-0166-1)

Keywords: Voriconazole, drug transporter, SLCO2B1, pharmacokinetics, pharmacogenomics

Student number: 2014-22029

TABLE OF CONTENTS

LIST OF FIGURES

LIST OF TABLES

LIST OF ABBREVIATIONS

AUC_{last}	Area under the concentration–time curve from 0 to last measurable time–point
AUC_{inf}	Area under the concentration–time curve from 0 to infinity
AUG_{0-4h}	Area under the glucose concentration–time curve for 4 hours
BMI	Body mass index
CI	Confidence interval
CL/F	Total apparent clearance
CL_{Cr}	Creatinine clearance
CL_R	Renal clearance
C_{max}	Maximum concentration of metformin
F	Bioavailability
F_{0-4h}	Bioavailability from 0 to 4 hours post–dose
GMR	Geometric mean ratio
IR	Immediate release formulation
OCT	Organic cation transporter
PCR	Polymerase chain reaction
PD	Pharmacodynamic

PK	Pharmacokinetic
SNP	Single nucleotide polymorphism
SST	Serum separating tube
$t_{1/2}$	Terminal half-life
T_{max}	Time to reach maximum concentration of metformin
V_d/F	Apparent volume of distribution
λ_z	Terminal elimination rate constant

INTRODUCTION

Invasive fungal infections, including aspergillosis, have caused significant medical problems, and are one of the leading causes of mortality in immunocompromised patients [1]. Voriconazole, a second-generation triazole, is one of the widely used antifungal agents for the prevention and treatment of invasive fungal infections [2, 3]. The use of voriconazole is, however, limited in some patients due to its adverse drug reactions, such as hepatotoxicity and central nervous system toxicity (visual disturbance, hallucinations, and altered mental status). These adverse reactions of voriconazole are closely related to its plasma concentrations [4]. The target trough concentration of voriconazole in plasma as recommended by British Society for Medical Mycology for the treatment of invasive fungal infections is between 1.0 and 5.5 mg/L [4, 5]. The plasma concentration of voriconazole, however, can widely vary among the individuals, and therefore, its efficient and safe use is often difficult [4, 6].

Voriconazole is primarily metabolized in the liver by the cytochrome P450 (CYP) enzymes (including CYP2C19, CYP2C9, and CYP3A4 isozymes). Genetic polymorphisms in CYP2C19 enzyme are one of the key factors that attribute to the inter-

individual variability of systemic voriconazole exposures [7–9]. CYP2C19 is the major metabolic enzyme that metabolizes voriconazole into its major inactive metabolite, voriconazole N-oxide. The CYP2C19 poor metabolizers (PMs) have demonstrated higher voriconazole systemic exposures than the intermediate metabolizers (IMs) or the extensive metabolizers (EMs) [9, 10]. The genetic polymorphisms in the CYP2C19 gene, however, can only explain 30–50% of the inter-individual variability in the systemic exposure of voriconazole, and many other contributing factors are still unexplained [11].

To identify the novel genetic variants affecting the pharmacokinetics (PK) of voriconazole, we have performed a pharmacogenomic analysis using the blood samples of the CYP2C19 PMs obtained from a previously performed clinical study (NCT01657201) [12], using a targeted Next-Generation Sequencing (NGS) pharmacogenomic panel [13]. From the NGS analysis, a total of 2,336 single nucleotide polymorphisms (SNPs) were identified. Among those SNPs, one (c.*396T>C, rs3781727) is located in the three-prime untranslated region (3'-UTR) of the solute carrier organic anion transporter family member 2B1 (SLCO2B1) gene. Its minor allele frequency (MAF) in the

Koreans is 29.3% and is significantly associated with the systemic voriconazole exposure [14], although this data needs to be validated in further in-vitro or in-vivo studies.

As voriconazole is also metabolized by the CYP3A4 enzyme, the functional variability of the CYP3A4 can be one of the factors attributing to the PK variability of voriconazole [8, 15]. Most of the CYP3A4 SNPs except for CYP3A4*22 are, however, known to have no clinically significant effect on the enzyme function. Further, the frequency of CYP3A4*22 is very rare in Asians [16]. Previous studies have indicated that the blood CYP3A4 messenger ribonucleic acid (mRNA) expression levels or urinary endogenous CYP3A metabolic biomarkers (6β-OH-cortisol/cortisol and 6β-OH-cortisone/cortisone) are related to the CYP3A enzyme activity [17-25]. It has been also demonstrated that the CYP3A5 enzyme function is closely related to the CYP3A4 enzyme function, whereas, the CYP3A5 SNP (CYP3A5*3) is not related to the PK of voriconazole [9, 16].

Based on these findings, the present study aimed to confirm the effects of SLCO2B1 c.*396T>C variant on the PK of voriconazole in the CYP2C19 PMs. Furthermore, the influence of the CYP3A4 enzyme activity on the PK of voriconazole was also

explored using CYP3A5 genotype, blood CYP3A4 mRNA expression levels, and urinary endogenous metabolic biomarkers. Additionally, we developed a population pharmacokinetic model of voriconazole based on our findings to further explore the influence of SLCO2B1 genotype on the pharmacokinetics of voriconazole after multiple administration.

METHODS

Subjects

Twelve healthy male subjects, aged between 20 and 45 years, with a body mass index in the range of 18.0 – 27.0 kg/m2, and all CYP2C19 PMs were enrolled in this study based on their SLCO2B1 c.*396T>C status [SLCO2B1 c.*396T>C wild-type and variant type (n = 6 or each type)]. To control the genetic factors except for SLCO2B1, only subjects who were CYP2C9 EMs and CYP3A4*22 non-carriers were enrolled to the study. Subjects with history of metabolic, hepatic, renal, hematological, pulmonary, cardiovascular, gastrointestinal, urological, endocrine, neurological, or psychiatric disorders that could have a significant effect on the PK of voriconazole were excluded from this study.

Clinical study design

This clinical study (NCT02906176) was approved by the Institutional Review Board of the Seoul National University Hospital, Seoul, Republic of Korea. The study was conducted in accordance to the principles of the Declaration of Helsinki, and

International Conference on Harmonisation of Technical Requirements for Pharmaceuticals for Human Use (ICH) Good Clinical Practice.

An open-label, single-dose, one-sequence, two-period, two-treatment, crossover study was performed (Figure 1). For genotyping of CYP2C19, CYP2C9, CYP3A4, CYP3A5, and SLCO2B1, the blood samples were obtained during a screening visit. The enrolled subjects received a single dose of voriconazole 200 mg intravenously (IV, infusion over 90 minutes) during the first period, and orally (with 150 mL of water) during the second period with a one-week washout between each dose.

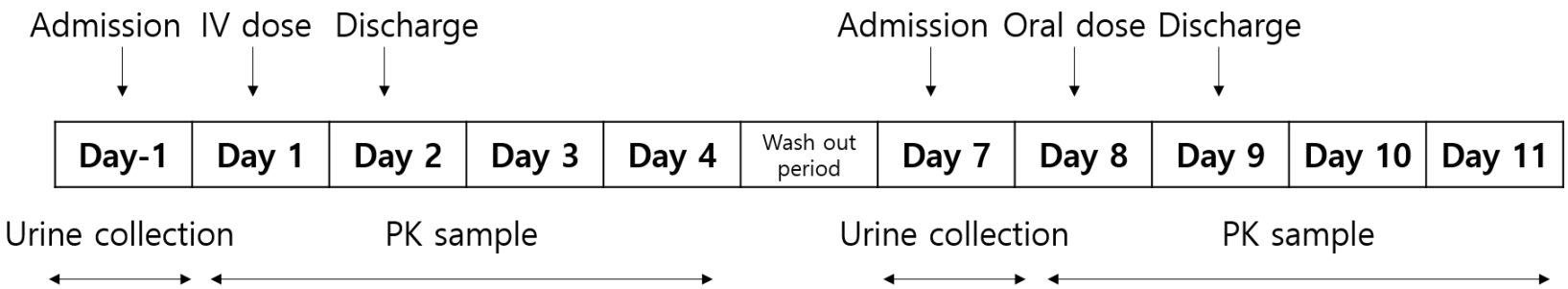

Figure 1. Study design. IV dose: Voriconazole 200 mg, Oral dose: Voriconazole 200 mg

Blood and urine collection

For voriconazole PK analysis, serial blood samples were collected in ethylenediaminetetraacetic acid tubes at 0 (i.e., pre-dose), 0.25, 0.5, 1, 1.5, 2, 3, 4, 6, 8, 12, 24, 48, and 72 h post-dose in each period. For measuring the CYP3A mRNA expression levels, whole blood samples were collected at pre-dose in each period. The interval urine samples were collected for 12 h before dosing in each period to analyse the endogenous CYP3A metabolic biomarkers.

Determination of the plasma concentration of voriconazole and voriconazole N-oxide

The quantitative analysis of voriconazole and voriconazole N-oxide was performed simultaneously using a high-performance liquid chromatography (Agilent 1260, Agilent Technologies, Santa Clara, CA, USA) and tandem mass spectrometry (API4000, SCIEX, Framingham, MA, USA) operated in a positive ionization mode. A Luna column (5 μm, C18, 2.0 mm x 100 mm, Phenomenex, Torrance, CA, USA) was used as a stationary phase, while the mobile phase consisted of 0.1% formic acid in

distilled water, and 0.1% formic acid in methanol (10:90, v/v) under an isocratic condition with a flow rate of 0.3 mL/min. The plasma samples were extracted using 100% methanol. Voriconazole-d3 was used as an internal standard. The concentration of voriconazole (or voriconazole N-oxide) was determined by computing the peak-area ratios of voriconazole (or voriconazole N-oxide) to voriconazole-d3 analysed in a multiple reaction monitoring (MRM) mode (m/z: 350.216→281.200 for voriconazole, m/z: 366.128→143.200 for voriconazole N-oxide, and m/z: 353.268→284.200 for voriconazole-d3). Linear calibration curves were established between the concentration range of 15 and 7500 ng/mL for both voriconazole and voriconazole N-oxide. The correlation coefficients (r) of the calibration curves were > 0.9966 for voriconazole and 0.9976 for voriconazole N-oxide. The intra- and inter-day precision results of the quality control samples for voriconazole were < 7.8% and 4.1%, respectively, and the intra- and inter-day accuracy results were approximately between 98.6–107.3% and 98.2–104.3%, respectively. The intra- and inter-day precision results of the quality control samples for voriconazole N-oxide were < 5.7% and 9.9%, respectively, and

the intra- and inter-day accuracy results were approximately between 99.3-108.9% and 95.9-100.5%, respectively.

Genotyping of CYP2C19, CYP2C9, CYP3A4, CYP3A5, and SLCO2B1

The DNA for genotyping was extracted from 200 μL of peripheral whole blood using a QIAamp DNA Blood Mini Kit (QIAGEN GmbH, Germany). The genotyping was performed using TaqMan allelic discrimination assays on a real time-polymerase chain reaction (PCR) System (Applied Biosystems®, Foster City, CA, USA). Ten microliters of PCR reaction mixture was prepared with 5 μL of 2X TaqMan Genotyping Master Mix, 0.5 μL of 20X Drug Metabolism Genotyping Assay Mix, 3.5 μL of DNase-free water, and 1 μL of DNA. The genotyping for the CYP2C19*2 (rs4244285, assay ID: C_25986767_70), CYP2C19*3 (rs4986893, assay ID: C_27861809_10), CYP2C9*3 (rs1057910, assay ID: C_27104892_10), CYP3A4*22 (rs35599367, assay ID: C_59013445_10), CYP3A5*3 (rs776746, assay ID: C_26201809_30), and SLCO2B1 (rs3781727, assay ID: C_27500327_10) SNPs was performed with validated TaqMan Genotyping Assays purchased from

Applied Biosystems. The PCR reactions were carried out as follows: initial denaturation at 95℃ for 10 min, 50 cycles for denaturation at 92℃ for 15 s, and anneal/extension at 60℃ for 1 min. The allelic discrimination results were determined after the amplification by performing an end-point read using a 7500 Real-Time PCR System software version 2.0.1 (Applied Biosystems, Foster City, CA, USA).

Estimation of CYP3A4 mRNA expressions in blood

The total RNA was extracted from the whole blood using a PAXgene Blood RNA Kit (PreAnalytiX). The complementary DNA (cDNA) was synthesized by the reverse transcription of 1 μg of total RNA using a QuantiNova Reverse Transcription Kit (Qiagen). A total of 15 μL of genomic DNA removal reaction was prepared with 2 μL of gDNA removal mix, 1 μL of internal control RNA, and 1 μg of RNA and RNase-free water. After incubation for 2 min at 45℃, 5 μL of a reverse-transcription Master Mix containing reverse transcription enzyme, buffer, and deoxynucleotides (dNTPs) were added to the genomic DNA removal reaction. The mixture was incubated for 20 min at 45℃, and the reverse transcriptase was inactivated for 5 min at 85℃.

A total of 20 μL of PCR reaction mixture was prepared with 10 μL of 2X QuantiNova SYBR Green PCR Master Mix (Qiagen), 2 μL QuantiTect Primer Assay (Qiagen), 6 μL of nuclease-free water, and 2 μL of complementary DNA. A real-time PCR was performed using CFX Connect Real-time PCR instrument (Bio-Rad, Hercules, CA, USA) as follows: initial denaturation at 95℃ for 2 min, 45 cycles for denaturation at 95℃ for 5 s, and anneal/extension at 60℃ for 10 sec. Glyceraldehyde 3-phosphate dehydrogenase (GAPDH) expression was used to normalize the CYP3A4 mRNA expression.

Pharmacokinetics data analysis

The PK parameters of voriconazole were determined by a non-compartmental analysis (NCA) using Phoenix WinNonlin software version 7.0 (Certara, St Louis, MO, USA). The area under the plasma concentration versus time curve (AUC) from 0 hour to the last measurable time (AUC_{last}) and AUC from 0 hour to 4 hour (AUC_{0-4h}) were determined using the linear trapezoidal method for the ascending concentrations and the log trapezoidal method for the descending concentration. The AUC_{0-4h} was used in this study to evaluate the PK change during the oral absorption

phase. The maximum concentration (C_{max}) and the time to reach C_{max} (T_{max}) were obtained from the observed values. The elimination rate constant (λ_z) was calculated using a linear regression of the log-linear portion of the plasma concentration-time curve, and the elimination half-life ($t_{1/2}$) was calculated as ln (2)/λ_z. The total clearance (CL) and apparent clearance (CL/F) were calculated using the ratio of the dose to the AUC. The volume of distribution (V_d) and apparent volume of distribution (V_d/F) were calculated as the CL (or CL/F) divided by λ_z. The metabolic ratios were calculated as AUC_{last} of voriconazole N-oxide/AUC_{last} of voriconazole. The AUC from time zero to infinity (AUC_{inf}) was calculated as AUC_{last} + Ct/λ_z, where Ct is the last measurable concentration. Bioavailability (F) was calculated as AUC_{inf} after oral dose/AUC_{inf} after IV dose, and F from 0 to 4 hours post-dose (F_{0-4h}) was calculated as AUC_{0-4h} after oral dose/AUC_{0-4h} after IV dose. The PK analysis set included all the subjects who completed the visit and received the study drug and have at least one evaluable post-dose PK concentration data. Actual sampling time was used to derive the PK parameters. Concentrations that were below the limit of quantification (BLQ) before T_{max} were treated as zero. However,

any concentrations that were BLQ after T_{max} were treated as a missing value. Missing values were excluded from the calculations.

Analysis of endogenous CYP3A metabolic biomarkers

The urinary concentrations of four steroids (6β-OH-cortisol, cortisol, 6β-OH-cortisone, and cortisone) were quantified using a 7890B series gas chromatography (Agilent Technologies, Santa Clara, CA, USA) coupled with a 7000B series triple quadrupole mass spectrometry (Agilent Technologies, GC-MS) following a previously described method [24]. Briefly, the four steroids were extracted from 2 mL of urine followed by solid-phase extraction, hydrolysis with β-glucuronidase, and liquid-liquid extraction. The extracted samples were evaporated using an N_2 evaporator, and the dried samples were derivatized with 40 μL of N-methyl-N-(trimethylsilyl) trifluoroacetamide. Finally, 3 μL of each sample was injected into the GC-MS for quantification. The CYP3A activities were estimated by the ratio of 6β-OH-cortisol/cortisol and 6β-OH-cortisone/cortisone [23-25].

Statistical analysis

All the demographic characteristics and PK parameters are expressed as the arithmetic mean and standard deviation (SD). Geometric mean ratios (GMRs) of the PK parameters and their 90% confidence intervals (CIs) for *SLCO2B1* c.*396T>C carriers (variant type) over non-carriers (wild type) were estimated using a general linear model. In this model, log-transformed PK parameters were used as dependent variables and genotype was used as a covariate. A non-parametric Mann-Whitney test was used to compare the PK parameters. A P value of < 0.05 was considered as statistically significant. All statistical analyses were performed using SAS software version 9.4 (SAS Institute Inc., Cary, NC, USA).

Population pharmacokinetic analysis

We used a logarithmically transformed voriconazole concentration data from the clinical trial to perform a population pharmacokinetic analysis using a non-linear mixed effect modelling approach with NONMEM (version 7.3.0, Icon Development Solutions, Ellicott City, MD, USA). To estimate the

pharmacokinetic parameters and their variabilities, a first-order conditional estimation method with the interaction option was employed.

The structure model was based on a known three-compartment models with a hypothetical inhibition compartment and a linear and/or non-linear elimination (i.e. Michaelis-Menten) model [26]. The absorption profile of oral voriconazole was described by a first-order process with a lag time, and the absolute bioavailability (F) was estimated using a logit model. The inter-individual variability for each pharmacokinetic parameter was evaluated using an exponential error model. An additive residual error model was used to describe the residual unexplained variability.

The effect of *SLCO2B1* genotype on the pharmacokinetics of voriconazole were tested using separate categories of VT referenced to WT. It was considered to be statistically significant when the objective function value (OFV) decreased > 3.84 ($p < 0.05$, χ^2 distribution with 1 degree of freedom). Only the biologically plausible parameter-covariate relationships were considered and included in the final model.

Model selection and validation

Throughout the model development process, model selection was evaluated based on the goodness of fit plots, the estimates, precision of parameters, and the decrease in OFV. The goodness of fit plots consisted of four plots as follows: observations versus population predictions, observations versus individual predictions, conditional weighted residual versus population predictions, and conditional weighted residuals versus time. The predictive performance of the model was assessed graphically by visual predictive checks (VPCs) performed by stratification of the *SLCO2B1* genotype (WT and VT) and rout of administration (IV and oral). The adequacy of the model was demonstrated by plotting the time course of the observations along with the prediction interval for the simulated values.

Model-based simulation

Based on the final parameter estimates of the developed model, model-based simulations were performed to predict the concentration profiles of voriconazole according to the *SLCO2B1* genotypes after multiple oral doses of different dosing regimens for CYP2C19 EM and PM subjects. For each CYP2C19 phenotype (EM and PM), 500 individual concentration-time profiles were simulated (A total of 1,000 individual concentration-time profiles). Each individual was randomly assigned to be either SLCO2B1 WT or VT. All parameters were fixed as the estimated values from the final model, including the inter-individual variabilities. For CYP2C19 PM subjects, $e^{-0.746}$ was multiplied to clearance (CL), and $e^{-0.44}$ was multiplied to fraction of clearance which cannot be explained (RCLP). For SLCO2B1 VT subjects, $e^{0.154}$, $e^{0.062}$, $e^{-0.0824}$, and $e^{0.0289}$ was multiplied to central volume of distribution (V2), clearance (CL), absorption rate constant (K_a), and bioavailability (F_1), respectively. The simulated dosing regimen was a standard oral dose (400 mg every 12 h on the first day followed by 200 mg every 12 h). The simulation was done for 7 days, which is considered sufficient to achieve the theoretical steady-state. Using the simulated voriconazole

concentration according to the *SLCO2B1* genotypes, the probability of attainment of the therapeutic target was calculated, where the target voriconazole trough concentration was predefines as the currently used therapeutic range of 2.0–5.5 mg/L [27, 28]. All simulation processes were carried out using NONMEM (version 7.3.0, Icon Development Solutions, Ellicott City, MD, USA).

RESULTS

Genotypes and demographic characteristics of the subjects

Twelve healthy male CYP2C19 PMs were enrolled and completed the study. Among them, six subjects were of the *SLCO2B1* wild-type (c.*396 TT) and the other six subjects were of the variant types [one with homozygous variant (c.*396 CC) and five with heterozygous variant (c.*396 TC)]. All the subjects were CYP2C9 EMs and were not carrying CYP3A4*22. One subject was CYP3A5 EM (*1/*1), five subjects were CYP3A5 IMs (*1/*3), and six subjects were CYP3A5 PMs (*3/*3) (Table 1).

The mean ± standard deviation (SD) of the different demographic characteristics of the *SLCO2B1* wild-type and variant types were as follows: 32 ± 6 vs. 27 ± 5 years (age), 178 ± 2 vs. 179 ± 7 cm (height), 71.4 ± 5.8 vs. 73.6 ± 8.5 kg (body weight), and 22.7 ± 1.8 vs. 23.1 ± 2.6 kg/m2 (body mass index), respectively. The demographic characteristics were not significantly different ($p > 0.05$) between the two *SLCO2B1* genotype groups (Table 2).

Table 1. Subjects' genetic status

Subject Number	SLCO2B1	CYP2C19	CYP2C9	CYP3A4*22	CYP3A5
AN101	c.*396TT	PM	EM	non-carrier	*1/*1
AN102	c.*396TT	PM	EM	non-carrier	*3/*3
AN103	c.*396TT	PM	EM	non-carrier	*1/*3
AN104	c.*396TT	PM	EM	non-carrier	*1/*3
AN105	c.*396TT	PM	EM	non-carrier	*1/*3
AN106	c.*396TT	PM	EM	non-carrier	*1/*3
AN201	c.*396TC	PM	EM	non-carrier	*3/*3
AN202	c.*396TC	PM	EM	non-carrier	*3/*3
AN203	c.*396TC	PM	EM	non-carrier	*3/*3
AN204	c.*396TC	PM	EM	non-carrier	*1/*3
AN205	c.*396CC	PM	EM	non-carrier	*3/*3
AN206	c.*396TC	PM	EM	non-carrier	*3/*3

EM, Extensive metabolizer; IM, Intermediate metabolizer; PM, poor metabolizer

Table 2. Demographic characteristics

		SLCO2B1 Wild Type (N = 6)	SLCO2B1 Variant Type (N = 6)	Total (N = 12)
Age (years)	Mean	32	26.83	29.42
	SD	5.97	4.71	5.79
	Range	24 – 41	20 – 31	20 – 41
BMI (kg/m2)	Mean	22.67	23.1	22.88
	SD	1.77	2.58	2.12
	Range	19.6 – 24.1	19.2 – 25.7	19.2 – 25.7
Height (m)	Mean	1.78	1.79	1.78
	SD	0.02	0.07	0.05
	Range	1.74 – 1.79	1.69 – 1.86	1.69 – 1.86
Weight (kg)	Mean	71.37	73.58	72.48
	SD	5.82	8.52	7.05
	Range	60.7 – 76.3	57.6 – 82.5	57.6 – 82.5

Effects of the SLCO2B1 genotype on the PK of voriconazole

The systemic exposure of voriconazole after its oral administration was lower in the *SLCO2B1* variant type group than the wild-type group **(Table 3 and Figure 2 – 4)**. The geometric mean (90% confidence interval) ratio [GMR (90% CI)] of the variant group to the wild-type group for the C_{max}, AUC_{last}, and AUC_{0-4h} of voriconazole were 0.76 (0.53– 1.08), 0.87 (0.61–1.25), and 0.89 (0.69–1.15), respectively. Furthermore, the inter-individual variations of these PK parameters were higher in the variant group **(Table 3 and Figure 4)**. The T_{max} was prolonged in the variant group as compared to the wild-type group while the $t_{1/2}$ did not show significant difference across the genotypes **(Table 3 and Figure 4)**. After intravenous administration of voriconazole, the AUC_{last} of voriconazole was also lower in the variant group as compared to the wild-type group, while the C_{max} and AUC_{0-4h} did not show much difference across the genotypes **(Figure 2, 3, and Table 3)**. While the metabolic ratios were higher ($p = 0.0130$) after oral administration compared to IV administration, they were similar across the genotypes regardless of the route of administration

(Table 3, Figure 5).

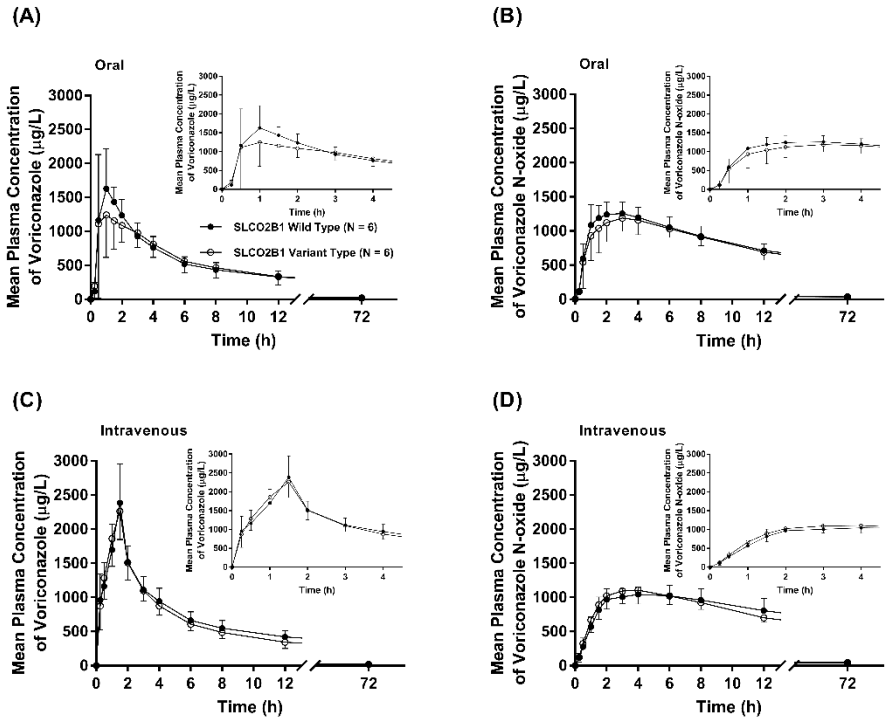

Figure 2. Mean plasma concentration–time profiles of voriconazole and voriconazole N–oxide after a single administration of voriconazole 200 mg up to 72 h post–dose (insets: up to 4 h post–dose) in the CYP2C19 poor metabolizers with *SLCO2B1* c.*396T>C (rs3781727) wild (filled circle) or variant (empty circle) genotype. The error bars denote the standard deviations. A and B: oral route, and C and D: intravenous route

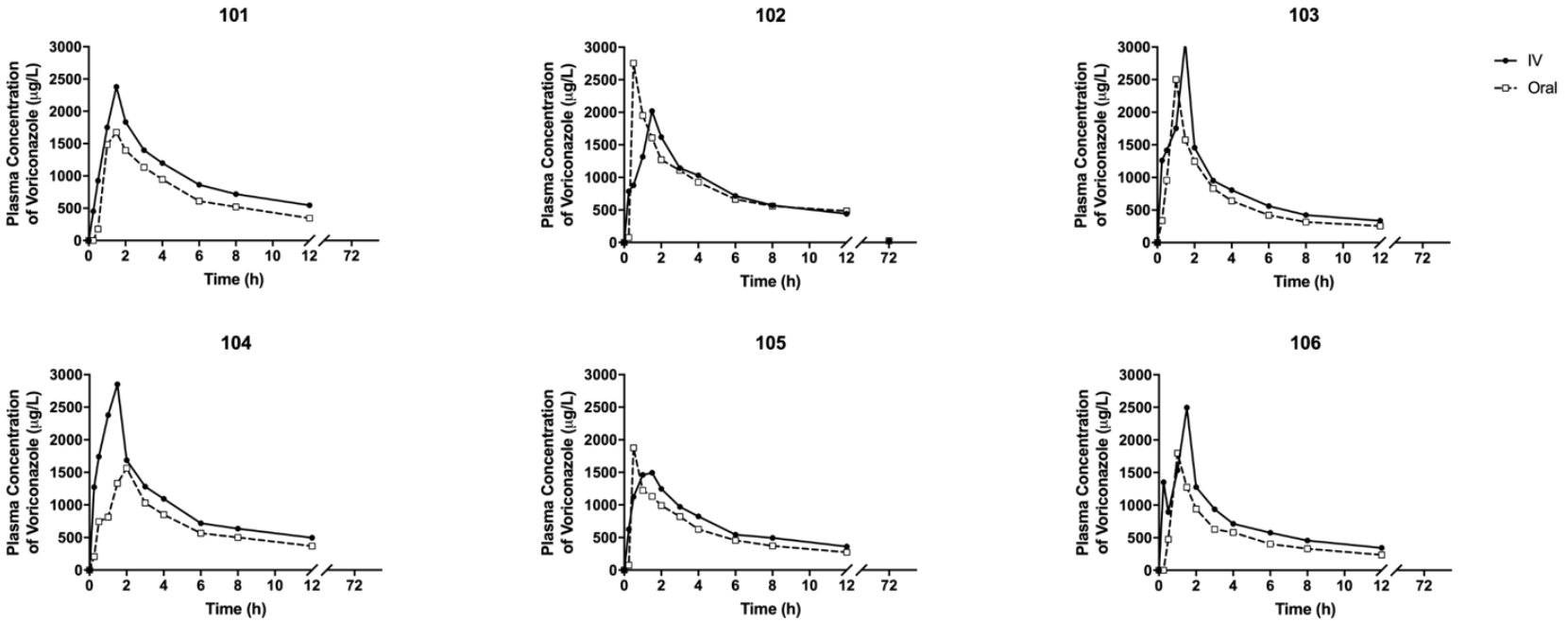

Figure 3-1. Individual plasma concentration-time profiles of voriconazole after a single administration of voriconazole 200 mg up to 72 h post-dose in the CYP2C19 poor metabolizers with SLCO2B1 c.*396T>C (rs3781727) wild (101-106) or variant (201-206) genotype. filled circle/solid-line: intravenous route, empty square/dashed-line: oral route.

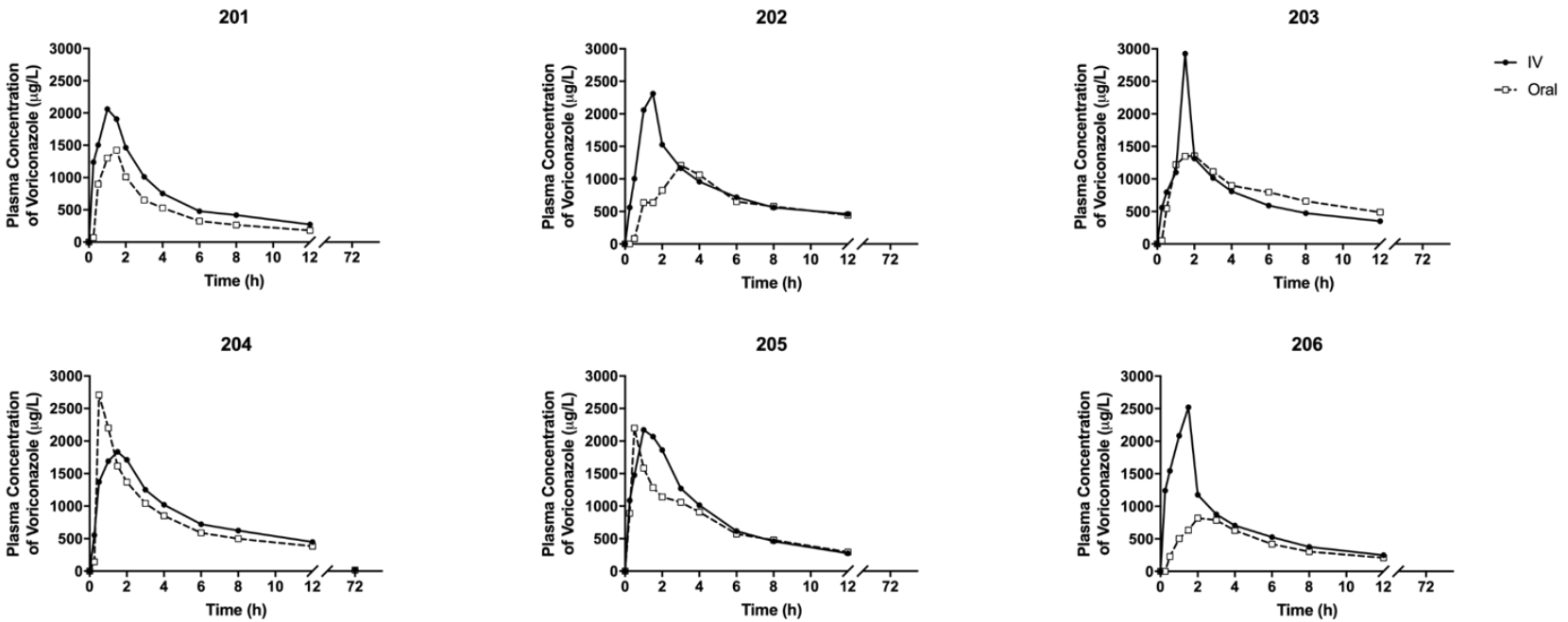

Figure 3-2. Individual plasma concentration−time profiles of voriconazole after a single administration of voriconazole 200 mg up to 72 h post−dose in the CYP2C19 poor metabolizers with SLCO2B1 c.*396T>C (rs3781727) wild (101−106) or variant (201−206) genotype. filled circle/solid−line: intravenous route, empty square/dashed−line: oral route.

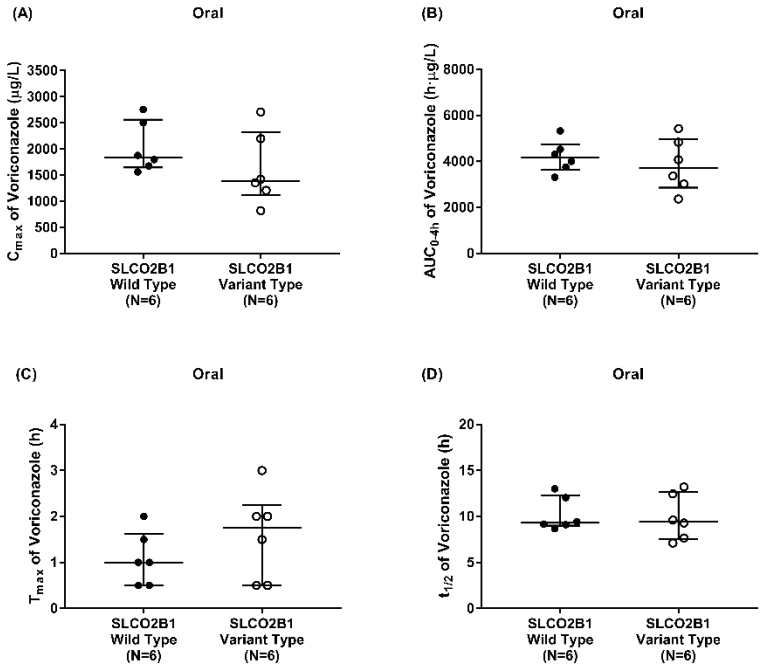

Figure 4. Individual pharmacokinetic parameters (C_{max}, AUC_{0-4h}, T_{max}, and $t_{1/2}$) after a single oral administration of voriconazole 200 mg in CYP2C19 poor metabolizers with *SLCO2B1* c.*396T>C (rs3781727) wild (filled circle) or variant (empty circle) genotype. The horizontal lines in the middle, top, and bottom represents the median, the 75th percentile, and the 25th percentile, respectively. (A) C_{max} by oral route. (B) AUC_{0-4h} by oral route. (C) T_{max} by oral route. (D) $t_{1/2}$ by oral route.

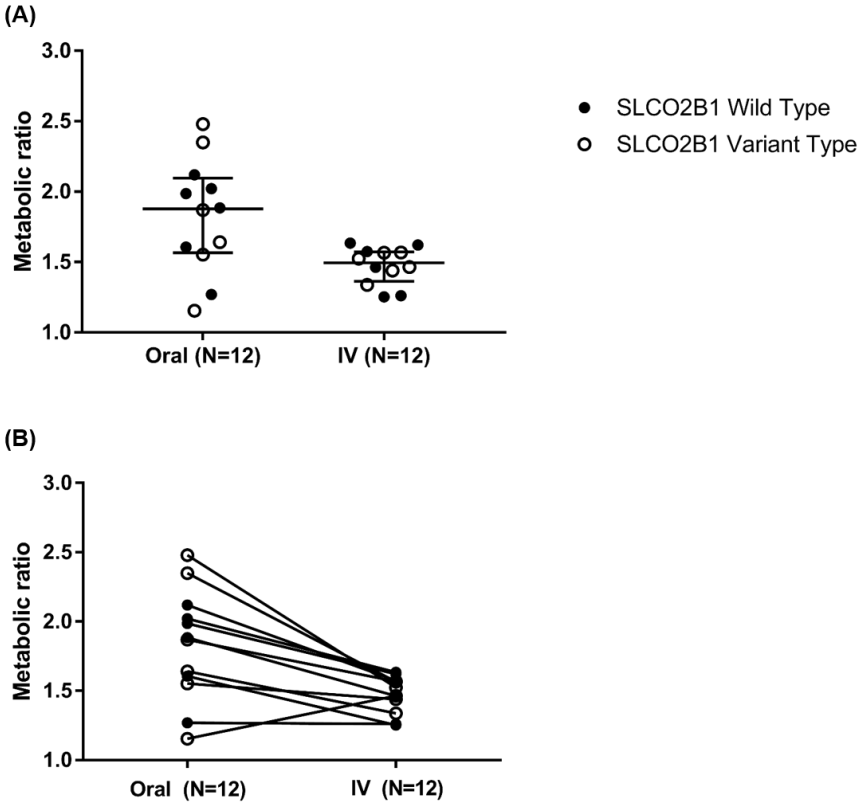

Figure 5. Individual metabolic ratio by rout of administration after administration of voriconazole 200 mg in CYP2C19 poor metabolizers with *SLCO2B1* c.*396T>C (rs3781727) wild (filled circle) or variant (empty circle) genotype. The horizontal lines in the middle, top, and bottom represents the median, the 75th percentile, and the 25th percentile, respectively. IV: intravenous

Table 3. The pharmacokinetic parameters of voriconazole and voriconazole N-oxide after a single oral and intravenous administration of voriconazole 200 mg in the cytochrome P450 2C19 poor metabolizers with *SLCO2B1* c.*396T>C (rs3781727) wild or variant genotypes

Route of administration	Parameters	Voriconazole			Voriconazole N-oxide		
		SLCO2B1 wild-type (n = 6)	SLCO2B1 variant type (n = 6)	GMR [90% CI]*	SLCO2B1 wild-type (n = 6)	SLCO2B1 variant type (n = 6)	GMR [90% CI]*
Intravenous	T_{max} (h)	1.50 [1.50 – 1.50]	1.50 [1.00 – 1.50]	–	4.00 [2.00 – 6.00]	4.00 [3.00 – 4.00]	–
	C_{max} (μg/L)	2384.50 ± 570.85 [23.9]	2303.83 ± 382.26 [16.6]	0.98 [0.78 – 1.23]	1085.85 ± 154.94 [14.3]	1116.53 ± 197.87 [17.7]	1.02 [0.87 – 1.20]
	AUC_{last} (h·μg/L)	16905.48 ± 3169.53 [18.7]	14930.75 ± 4168.27 [27.9]	0.86 [0.68 – 1.11]	24509.16 ± 3520.37 [14.4]	21872.13 ± 4967.61 [22.7]	0.88 [0.73 – 1.07]
	AUC_{0-4h} (h·μg/L)	5411.20 ± 812.04 [15.0]	5396.38 ± 421.90 [7.8]	1.00 [0.89 – 1.14]	3077.30 ± 474.50 [15.4]	3341.46 ± 659.06 [19.7]	1.08 [0.91 – 1.28]
	$t_{1/2}$ (h)	11.04 ± 2.27 [20.6]	10.23 ± 2.87 [28.1]	–	12.20 ± 2.20 [18.0]	10.71 ± 2.55 [23.8]	–
	CL (L/h)	11.78 ± 2.18 [18.5]	13.42 ± 3.23 [24.1]	–	–	–	–
	Metabolic ratio**	–	–	–	1.47 ± 0.17 [11.6]	1.48 ± 0.09 [6.1]	–
Oral	T_{max} (h)	1.00 [0.50 – 2.00]	1.75 [0.50 – 3.00]	–	2.00 [1.00 – 3.00]	3.50 [1.50 – 4.00]	–
	C_{max} (μg/L)	2027.67 ± 483.08 [23.8]	1619.27 ± 698.46 [43.1]	0.76 [0.53 – 1.08]	1314.83 ± 185.85 [14.1]	1231.92 ± 223.39 [18.1]	0.93 [0.78 – 1.11]
	AUC_{last} (h·μg/L)	13373.42 ± 4220.17 [31.6]	11982.11 ± 4508.32 [37.6]	0.87 [0.60 – 1.25]	23250.79 ± 3011.77 [13.0]	20570.15 ± 5314.13 [25.8]	0.87 [0.70 – 1.07]
	AUC_{0-4h} (h·μg/L)	4209.45 ± 695.11 [16.5]	3849.54 ± 1150.12 [29.9]	0.89 [0.69 – 1.15]	4176.52 ± 541.19 [13.0]	3826.55 ± 1007.10 [26.3]	0.90 [0.72 – 1.11]
	$t_{1/2}$ (h)	10.17 ± 1.86 [18.3]	9.90 ± 2.50 [25.3]	–	11.16 ± 2.27 [20.3]	10.78 ± 2.97 [27.6]	–
	CL/F (L/h)	15.58 ± 4.05	16.90 ± 6.08	–	–	–	–

	[26.0]	[35.9]				
F (%)	77.9 ± 13.6 [17.4]	82.5 ± 14.3 [17.3]	–	–	–	–
F_{0-4h} (%)	78.9 ± 15.9 [20.2]	71.3 ± 20.3 [28.5]	–	–	–	–
Metabolic ratio**	–	–	–	1.81 ± 0.32 [17.7]	1.84 ± 0.50 [27.2]	–

Data presented as mean ± standard deviation [coefficient of variation %] except for T_{max}, which is presented as median [minimum – maximum].

*Geometric mean ratio (GMR) and 90% confidence intervals (CI) of the *SLCO2B1* variant type to the *SLCO2B1* wild-type for C_{max}, AUC_{last}, and AUC_{0-4h}

**Metabolic ratio was calculated as the AUC_{last} of N-oxide voriconazole divided by the AUC_{last} of voriconazole

Effects of CYP3A activity on the PK of voriconazole

The CYP3A activity measured in this study did not show any significant association with the N-oxide metabolism of voriconazole. The blood CYP3A4 mRNA expressions and the endogenous CYP3A activity biomarkers (6β-OH-cortisol/cortisol and 6β-OH-cortisone/cortisone) exhibited no statistically significant correlation with the metabolic ratio of voriconazole (Figure 6). The metabolic ratios were also not significantly different across the CYP3A5 genotypes (Figure 6).

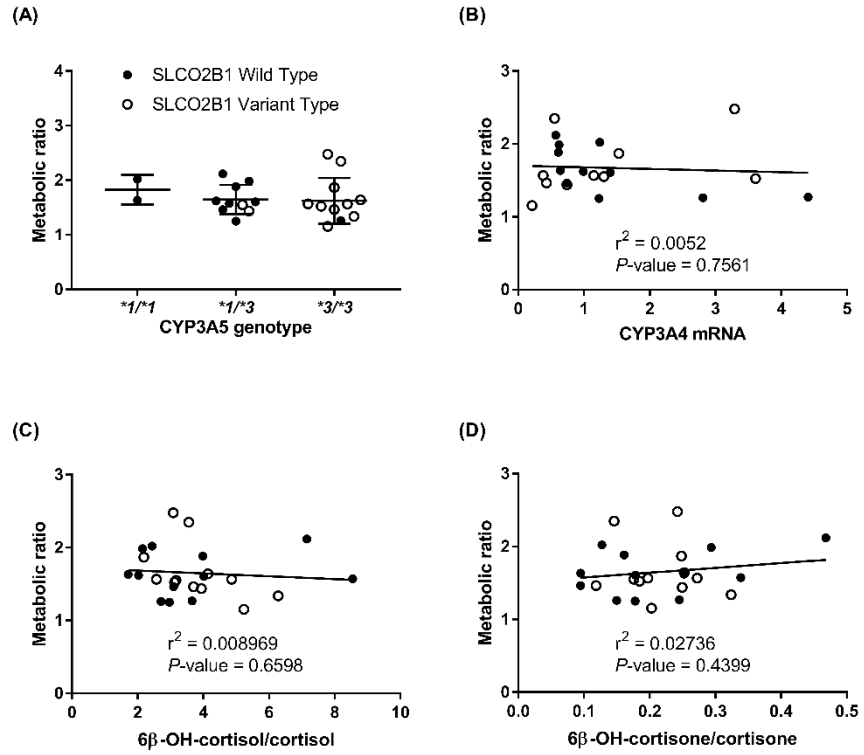

Figure 6. Relationship between the individual metabolic ratio and CYP3A4 activity biomarkers after a single (intravenous or oral) administration of voriconazole 200 mg in CYP2C19 poor metabolizers with *SLCO2B1* c.*396T>C (rs3781727) wild (filled circle) or variant (empty circle) genotype. (A) relationship between the individual metabolic ratio and CYP3A5 genotype. (B) relationship between the individual metabolic ratio and CYP3A4 relative baseline (trough) mRNA expression. (C) relationship between the individual metabolic ratio and baseline (trough) 6β-OH-cortisol/cortisol. (D) relationship between the individual metabolic ratio and baseline (trough) 6β-OH-cortisone/cortisone.

Population pharmacokinetic model

A three-compartment model with a first-order oral absorption, an absorption lag time, and elimination along with an inhibition compartment model appropriately described the time-concentration profile of voriconazole, showing distinct non-linear pharmacokinetic behavior.

Since our data was based on 12 healthy subjects, while the original model was developed using approximately 200 subject data (patients and healthy subjects), the model was overcomplicated for our data. Therefore, some of the parameters were fixed with known values from a previous report [26]. The *SLCO2B1* genotype did not turn out to be a statistically significant covariate for the PK parameters. However, this was somewhat expected since *SLCO2B1* genotype did not show statistically significant effect on the PK of voriconazole based on the NCA from the clinical trial. For exploratory reasons, we have incorporated fixed values (estimated values from covariate analysis) to central volume of distribution (V2), clearance (CL), absorption rate constant (K_a), and bioavailability (F1). The NONMEM control code for the final model was as follows:

```
$SUBROUTINES ADVAN6 TOL=5

$MODEL
COMP=(DEPOT)
COMP=(CENTRAL)
COMP=(PERIPH1)
COMP=(PERIPH2)
COMP=(INHIBIT)

$PK
IF(GENO.EQ.0) THEN ; RM/EM
GENOF=0
GENOF1=0
ENDIF

IF(GENO.EQ.1) THEN ; IM
GENOF=THETA(17)
GENOF1=THETA(19)
ENDIF

IF(GENO.EQ.2) THEN ; PM
GENOF=THETA(18)
GENOF1=THETA(20)
ENDIF

IF(GRADE.GE.3) THEN ; GRADE 3&4
LFF=THETA(24)
ELSE
LFF=0
ENDIF

IF(SLCO.EQ.0) THEN ; WT
SLCOV=0
SLCOC=0
SLCOK=0
SLCOF=0

ENDIF

IF(SLCO.EQ.1) THEN; VT
```

```
SLCOV=THETA(25)
SLCOC=THETA(26)
SLCOK=THETA(27)
SLCOF=THETA(28)

ENDIF

TVV2 = THETA(1) * EXP(SLCOV) ;SLCO~V
TVCL = THETA(2) * (WT/70)**THETA(16) * EXP(GENOF) *
EXP(LFF) * EXP(SLCOC) ;SLCO~C
TVV3 = THETA(3) * (WT/70)**THETA(15)
TVQ2 = THETA(4) * (WT/70)**THETA(21)
TVV4 = THETA(5)
TVQ3 = THETA(6)
TVKA = THETA(7) * EXP(SLCOK) ;SLCO~K
TVF1 = THETA(8) * EXP(SLCOF) ;SLCO~F

V2 = TVV2 * EXP(ETA(1))
CL = TVCL * EXP(ETA(2))
V3 = TVV3 * EXP(ETA(3))
Q2 = TVQ2 * EXP(ETA(4))
V4 = TVV4
Q3 = TVQ3
KA = TVKA * EXP(ETA(5))
LGF1 = LOG(TVF1/(1-TVF1)) + ETA(6)
F1 = EXP(LGF1) / (1 + EXP(LGF1))
ALAG1 = THETA(9) * EXP(ETA(7))

RCLF = THETA(10) * EXP(GENOF1)* EXP(ETA(8))
IC50 = THETA(11)
KIC = THETA(12)

KE = CL/V2
K23 = Q2/V2
K32 = Q2/V3
K24 = Q3/V2
K42 = Q3/V4
S2 = V2/1000

$DES
CONC=A(2)/V2
```

```
INH= RCLF + (1-RCLF)*(1 - A(5)/(IC50 + A(5)))

DADT(1) = -KA*A(1)
DADT(2) = KA*A(1) -KE*A(2)*INH - K23*A(2) +
K32*A(3) -K24*A(2) + K42*A(4)
DADT(3) = K23*A(2) - K32*A(3)
DADT(4) = K24*A(2) - K42*A(4)
DADT(5) = KIC*(CONC-A(5))

$ERROR
IPRED=0
IF(F.GT.0) IPRED=LOG(F)
IF(PART.EQ.5) THEN
W = SQRT(THETA(22)**2*IPRED**2 + THETA(23)**2)
ELSE
W = SQRT(THETA(13)**2*IPRED**2 + THETA(14)**2)
ENDIF

Y = IPRED + W*EPS(1)
IRES = DV-IPRED
IWRES = IRES/W

$THETA
(0, 35.6) ; V2
(0, 45.2) ; CL
(0, 56.6) ; V3
(0, 10.3) ; Q2
(25.4) FIX; V4
(54.6) FIX; Q3
(0, 1.24) ; KA
(0, 0.859,1) ; F1
(0, 0.235) ; ALAG1
(0.162) FIX;RCLF
(0.01) FIX ; IC50
(0.002) FIX;KIC
(0.0001) FIX ; Prop.RE (sd)
(0, 0.31) ; Add.RE (sd)
(0, 2.2) FIX ; WT~V3
(0, 0.595) FIX ; WT~CL
(-0.186) FIX ; IM~CL
(-0.746) FIX ; PM~CL
(-0.51) FIX ; IM~RCLF
```

```
(-0.44) FIX ; PM~RCLF
(0, 2.56) FIX; WT~Q2

(0.0001) FIX ; Prop.RE (sd) PART5
(0.799) FIX; Add.RE (sd) PART5
(-0.75) FIX; GRADE>=3~CL

(0.154) FIX; SLCO~V2
(0.062) FIX; SLCO~CL
(-0.0824) FIX; SLCO~Ka
(0.0289) FIX; SLCO~F1

$OMEGA BLOCK(2)
0.109 ; IIV V2
0.0346 0.128 ; IIV CL


$OMEGA
0 FIX; IIV V3
0 FIX; IIV Q2
0.65 ; IIV KA
0.179 ; IIV F1
0 FIX ; IIV ALAG1
0.4 FIX; IIV RCLF

$SIGMA
1 FIX

$EST METHOD=1 INTER MAXEVAL=9999 NOABORT SIG=2
PRINT=1 POSTHOC

$COV

$TABLE ID NTIME TIME NTAD TAD AMT RATE DV MDV
EVID CMT PRD TRT PART IPRED IWRES CWRES
ONEHEADER NOPRINT FILE=sdtab1045

$TABLE V2 CL V3 Q2 KA F1 ALAG1 V4 Q3 RCLF IC50 KIC
ETA1 ETA2 ETA3 ETA4 ETA5 ETA6 ETA7 ETA8
ONEHEADER NOPRINT FILE=patab1045
```

$TABLE ID AGE WT HT BMI ALP AST ALT GGT CRE GFR ONEHEADER NOPRINT FILE=cotab1045

$TABLE ID GENO SEX VPC TDM CON PPI USE LFT GRADE

SLCO ONEHEADER NOPRINT FILE=catab1045

The absorption rate constant of $1.22h^{-1}$ and the lag time of 0.236h appropriately describe the absorption phase of orally administered voriconazole. The absorption oral bioavailability of voriconazole was estimated to be 86%. The estimated typical CL of voriconazole was 48.1 L/h. Most of the typical parameter values were estimated with a good precision (Table 4).

Table 4. Parameter estimates of the final population pharmacokinetic model.

Parameters	Estimates	RSE (%)
Structural model		
V2; central volume of distribution (L)	27.8	19
CL; clearance (L/h)	48.1	4
V3; peripheral 1 volume of distribution (L)	58.1	7
Q2; inter-compartmental clearance between central and peripheral 1 compartment (L/h)	16.3	12
V4; peripheral 2 volume of distribution (L)	25.4 FIX	NA
Q3; inter-compartmental clearance between central and peripheral 2 compartment (L/h)	54.6 FIX	NA
K_a; absorption rate constant (h^{-1})	1.22	33
F_1; bioavailability	0.86	4
$ALAG_1$; absorption lag-time (h)	0.236	2
RCLP; fraction of clearance which cannot be inhibited	0.162 FIX	NA
IC_{50}; concentration in the inhibition compartment yielding 50% of maximum clearance inhibition	0.01 FIX	NA
K_{IC}; rate constant into inhibition compartment	0.002 FIX	NA
Inter-individual variability (IIV)		
IIV for V2 (% CV)	44.1	36[a]
IIV for CL (% CV)	12.1	14[a]
IIV for V3 (% CV)	0 FIX	NA[a]
IIV for Q2 (% CV)	0 FIX	NA[a]
IIV for Ka (% CV)	114.1	28[a]
IIV for F1 (% CV)	83.4	39[a]
IIV for ALAG1 (% CV)	0 FIX	NA[a]
IIV for RCLF (% CV)	70.1 FIX	NA[a]

Residual variability		
Additive error for healthy subjects (mg/L)	0.224	8
Additive error for patients (mg/L)	0.799 FIX	NA

[a] Standard error given on the variance scale; [b] Standard error of the covariance estimate.

Model validation

The basic goodness of fit (Figure 7) and VPC plots (Figure 8) showed a good predictive performance of the developed model and indicated that the model appropriately described the observed voriconazole concentration in accordance with the *SLCO2B1* genotypes.

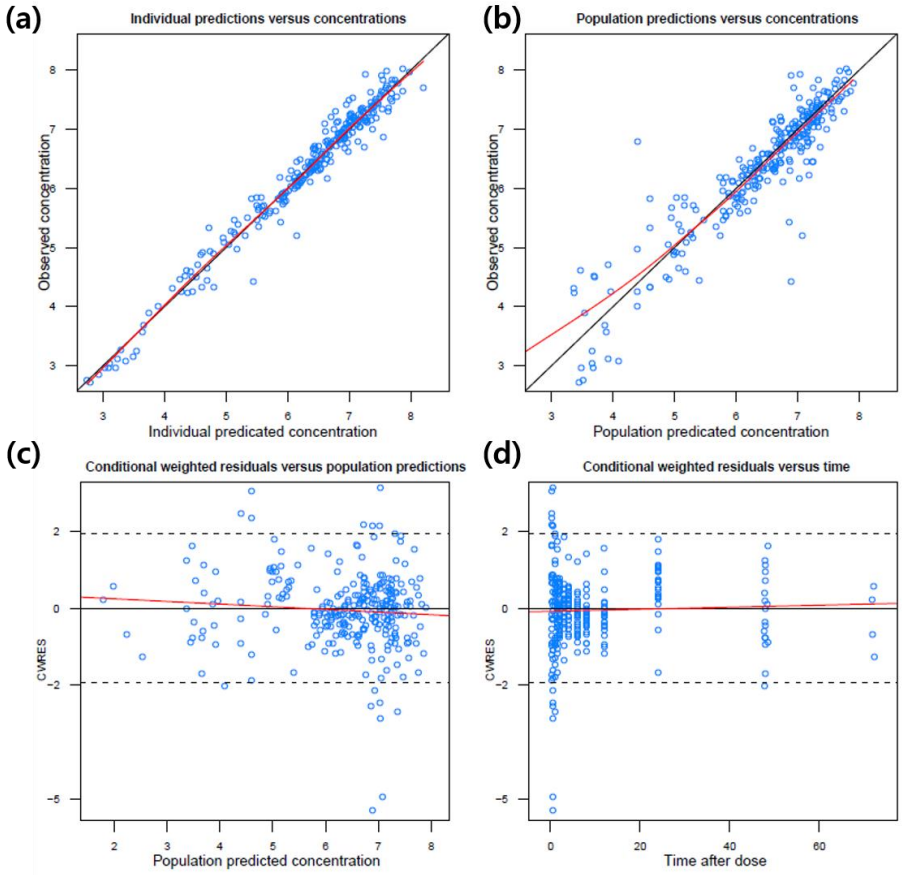

Figure 7. Basic goodness-of-fit plots of final population pharmacokinetic model for voriconazole. (a) observations versus population predicted concentration; (b) observations versus individual predicted concentration; (c) conditional weighted residuals (CWRES) versus population predicted concentration; (d) conditional weighted residuals (CWRES) versus time after dose

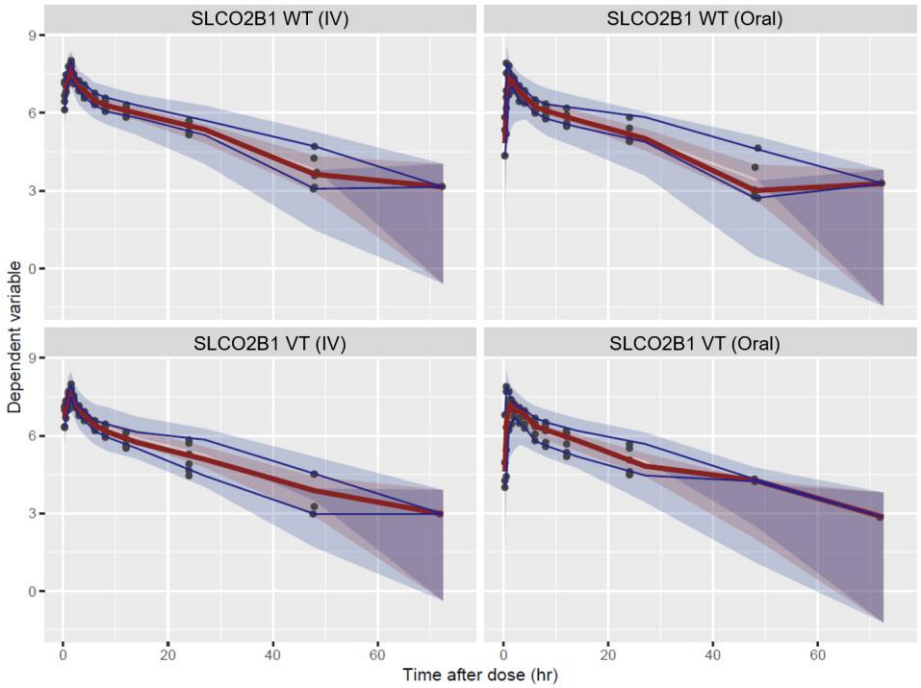

Figure 8. Visual predictive check for *SLCO2B1* wild types (WT) and *SLO2B1* variant types (VT) in the final pharmacokinetic model by rout of administration. The circles represent the observed concentrations. The lines represent the median (red) and the 5^{th} and 95^{th} percentiles (blue) of the observed concentration. The areas represent the 95% confidence intervals for the median (red) and 90% prediction interval (blue) of the simulated concentrations.

Simulation of standard dosing regimen according to the SLCO2B1 genotype in CYP2C19 EMs and PMs

Based on the final population pharmacokinetic model, the concentration–time profiles of voriconazole after 7–day multiple oral doses of standard dosing regimen (400 mg twice daily for two doses followed by 200 mg twice daily) were simulated according to the *SLCO2B1* genotypes in CYP2C19 EMs and PMs **(Figure 9)**. When classified according to the *SLCO2B1* genotypes, the trough concentrations reached mostly below the target range (2.0–5.5 mg/L) for both *SLCO2B1* WT and VT in CYP2C19 EMs. In CYP2C19 PMs, the trough concentrations were within the target range regardless of the *SLCO2B1* genotype.

The probabilities of reaching subtherapeutic concentration were higher in *SLCO2B1* VT (73%) compared to WT (68%) in CYP2C19 EMs. Meanwhile, the probabilities of reaching therapeutic concentration (*SLCO2B1* WT: 24%, *SLCO2B1* VT: 22%) and toxic concentrations (*SLCO2B1* WT: 7%, *SLCO2B1* VT: 5%) were higher in *SLCO2B1* WT compared to *SLCO2B1* VT in CYP2C19 EMs. **(Figure 10)**.

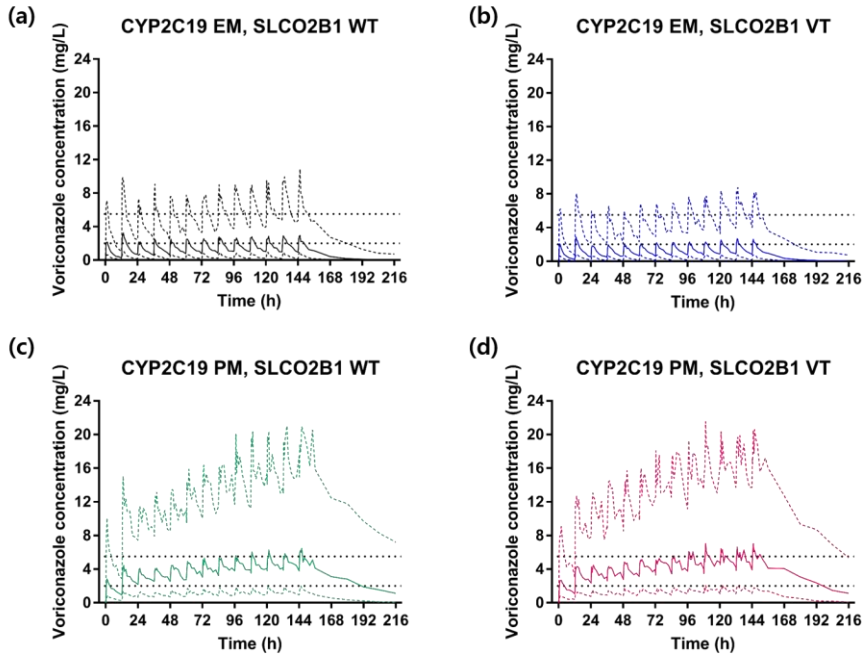

Figure 9. Predicted median concentration–time profile over the first 7 days of treatment of total 1,000 simulated patients. (a) CYP2C19 EM and SLCO2B1 WT; (b) CYP2C19 EM and *SLCO2B1* VT; (c) CYP2C19 PM and *SLCO2B1* WT; (d) CYP2C19 PM and *SLCO2B1* VT. Standard oral dosing (400 mg twice daily for two doses followed by 200 mg twice daily) was used. The solid lines represent the median, with the dotted lines representing the 10^{th} and 90^{th} percentiles. The horizontal dotted lines represent the therapeutic target range for voriconazole trough plasma concentration of 2.0 to 5.5 mg/L.

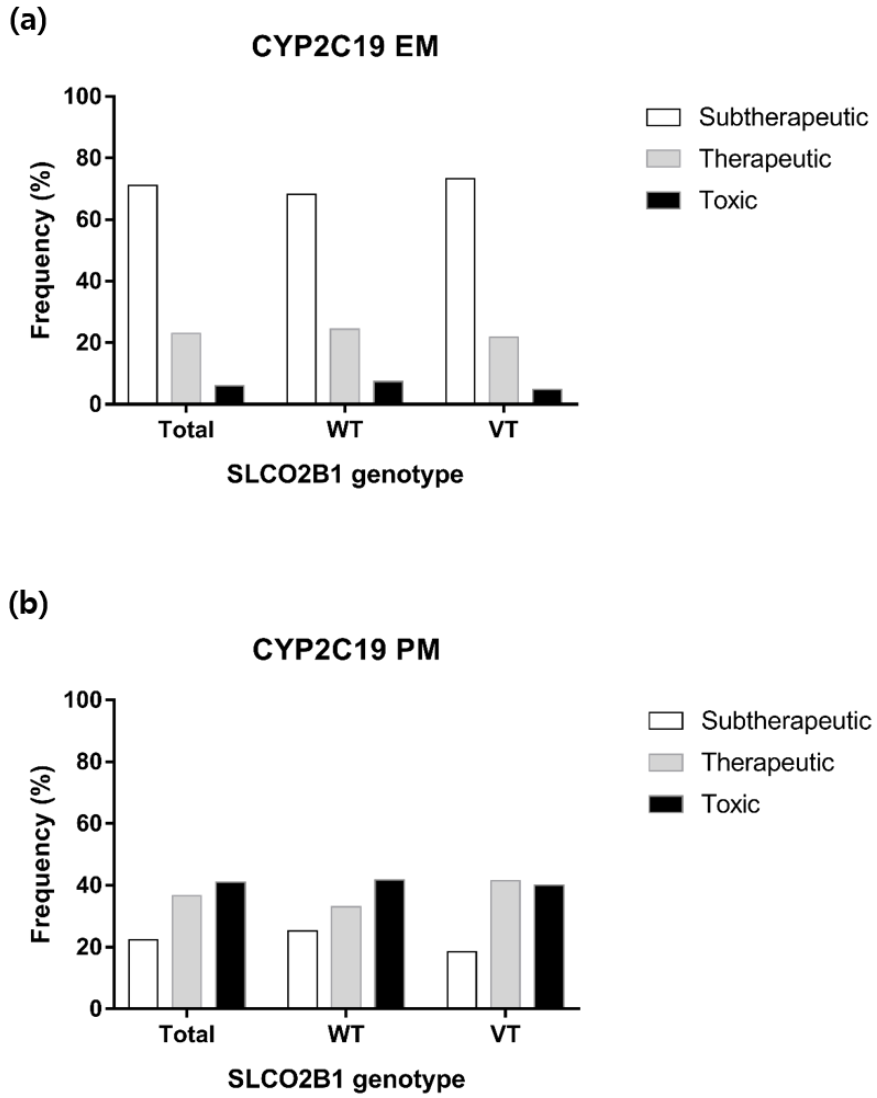

Figure 10. Probability of voriconazole therapeutic target attainment from model-based simulations of voriconazole pharmacokinetic profiles after the following voriconazole standard oral dosing regimens on day 7 (400 mg twice daily for two doses followed by 200 mg twice daily); (a) CYP2C19 EM; (b) CYP2C19 PM. Therapeutic target range for voriconazole trough plasma concentration was from 2.0 to 5.5 mg/L.

DISCUSSION

To maximize the influence of *SLCO2B1* c.*396T>C variant on the PK of voriconazole, only the CYP2C19 PMs were included in this study. Several confounding factors apart from the genetic status of CYP2C19, such as disease status, co-medications (CYP inducers and inhibitors), foods, and herbal medicines (e.g., St John's-wort), however, can increase the inter-patient PK variability of voriconazole [2, 29, 30]. Genetic polymorphisms in the metabolizing enzymes apart from CYP2C19, such as CYP2C9 and CYP3A4 or in the drug transporters may also add to the PK variability of voriconazole. To control these possible confounding factors, this study was performed only with the healthy subjects who were CYP2C9 EMs and carrying a CYP3A4*22 wild-type, and the use of co-medications was strictly controlled.

In this study, the systemic exposure of voriconazole were decreased in the subjects with a *SLCO2B1* c.*396T>C variant than the subjects carrying a wild-type, although it failed to reach a statistical significance. The C_{max}, AUC_{last}, and AUC_{0-4h} of voriconazole were lower in the variant group compared to the wild-type group with higher inter-individual variations.

Furthermore, the T_{max} of voriconazole was prolonged in the variant group compared to the wild-type group, while the $t_{1/2}$ did not show much difference (Table 3 and Figure 3). It suggests that the rate and extent of oral absorption of voriconazole was decreased in the variant group than the wild-type group.

An influx transporter, organic anion transporting polypeptide 2B1 (OATP2B1) is encoded by the *SLCO2B1* gene and is expressed in various tissues in the human body including placenta, heart, skeletal muscle, liver, and intestine [31, 32]. To the best of our knowledge, studies evaluating the clinical implications of *SLCO2B1* c.*396T>C SNP are sparse. It has been revealed that the OATP2B1 has an important role in the oral absorption of statins, and the inhibition of OATP2B1 can significantly reduce the systemic exposure of rosuvastatin in human [33]. Moreover, several clinical studies have reported the associations of *SLCO2B1* SNP with the PK and response of its substrate drugs. The *SLCO2B1* c.1457C>T SNP was shown to decrease the exposure of fexofenadine, and c.935G>A SNP was associated with a decreased montelukast plasma concentration leading to a poor drug response [34, 35]. The *SLCO2B1* c.*396T>C SNP is located in the 3'-UTR region of the *SLCO2B1*

gene, and this SNP is capable of altering the OATP2B1 transporter functions in human. Specifically, the *SLCO2B1* c.*396T>C SNP may decrease the OATP2B1 functions in the human intestine, thereby reducing the systemic absorption of voriconazole in the individuals carrying the variant type. Although the difference in AUC_{last} was greater than that of AUC_{0-4h} between *SLCO2B1* wild-type and variant-type group, the differences in C_{max} and AUC_{0-4h} of voriconazole between the two groups were greater when voriconazole was administered orally compared to an intravenous route **(Table 3 and Figure 4)**. Therefore, the claim that the absorption of voriconazole may have been affected by *SLCO2B1* genotype cannot be dismissed. Additionally, this study was conducted in subjects with the same CYP2C19, CYP2C9, and CYP3A4*22 genotypes, implying that the *SLCO2B1* genotype is most likely responsible for these results.

The F_{0-4h} of voriconazole was reduced in *SLCO2B1* variant-type compared to wild-type group, while it was not the case for F. This suggests that while SLCO2B1 genotype may affect the absorption of voriconazole initially, its effect may be reduced over time. This could be explained by the fact that

voriconazole could potentially cross cell membranes via passive diffusion since it is a lipophilic compound of moderate size with no net charge at physiological pH values [3, 39].

The CYP3A4 activity biomarkers evaluated in this study could not explain the additional PK variabilities of voriconazole beside the CYP2C19 genetic status (Figure 6). The CYP3A4 enzyme activity is highly variable among the individuals and its variability cannot be explained by the common genetic variations [36]. The CYP3A4*22 is a well-known allele that causes loss of function of the CYP3A4 enzyme, but its frequency is rare in the general populations as well as in Asians [16]. The CYP3A5*3 is another important SNP that affects the total CYP3A subfamily enzyme function [16]. The CYP3A5*3 was, however, not related to the voriconazole plasma concentration in this study. This finding is consistent with other previous reports [9, 16]. In addition, based on some earlier studies, we expected that the CYP3A4 mRNA expression level in blood or the urinary endogenous steroid ratios could represent the CYP3A4 activity in human [17-25]. Our study result, however, may indicate that the variability of the CYP3A4 activity dose not significantly affect

voriconazole N-oxidation when the other metabolizing pathway (e.g. CYP2C9) is still functional.

The metabolic ratio of voriconazole was increased when administered orally, regardless of the *SLCO2B1* genotype. It is reasonable to assume that the increased metabolic ratio is due to the first-pass metabolism of voriconazole. First-pass metabolism may occur in the liver or intestine, and CYP3A4 is the predominant enzyme (approximately 80%) expressed in the small intestine [37]. Therefore, if metabolism in the intestine was a significant factor in the first-pass metabolism, CYP3A4 would have been the major source of the metabolism. However, in our study, the CYP3A4 activity did not affect the metabolism of voriconazole which implies that the intestinal CYP3A4 did not play a significant role in the increased metabolic ratio after oral administration. This is consistent with a previous physiologically based pharmacokinetic model study that suggested voriconazole is not subject to intestinal first-pass metabolism in adults [38].

This study had some major limitations. First, due to the exploratory nature, the study was conducted in a limited number of subjects. As a result, we could not show statistically significant difference in PK parameters between the two

genotype groups, and the simulation results based on the final population PK model did not show *SLCO2B1* genotype having a drastic effect on the probability of reaching therapeutic range in CYP2C19 EMs. Secondly, only CYP2C19 PM males were enrolled in the clinical study, while the effects of *SLCO2B1* genotype on the PK of voriconazole in CYP2C19 EMs and female subjects are unknown. Consequently, the simulation results may not properly predict the time–concentration profile of voriconazole in CYP2C19 EMs and/or female subjects. Therefore, further studies with greater sample size including variety of subjects (e.g. CYP2C19 EM, female) are warranted to confirm our hypothesis. However, we believe our clinical study could serve as an early proof of concept study.

CONCLUSION

In conclusion, the oral absorption of voriconazole was decreased and delayed in the subjects with a *SLCO2B1* c.*396T>C variant compared to the wild-type. This finding suggests that the *SLCO2B1* c.*396T>C may be associated with a reduced function of the intestinal OATP2B1, and thereby attributing to the inter-individual PK variability of voriconazole. Further studies in a bigger pool of patients will be helpful to evaluate the clinical importance of the *SLCO2B1* c.*396T>C genetic polymorphism with regard to the safety and efficacy of voriconazole.

REFERENCES

1. Pfaller MA, Pappas PG, Wingard JR. Invasive Fungal Pathogens: Current Epidemiological Trends. Clinical Infectious Diseases 2006; 43: S3-S14.

2. Johnson LB, Kauffman CA. Voriconazole: a new triazole antifungal agent. Clinical infectious diseases : an official publication of the Infectious Diseases Society of America 2003; 36: 630-7.

3. Levêque D, Nivoix Y, Jehl F, Herbrecht R. Clinical pharmacokinetics of voriconazole. International journal of antimicrobial agents 2006; 27: 274-84.

4. Pound MW, Townsend ML, Dimondi V, Wilson D, Drew RH. Overview of treatment options for invasive fungal infections. Medical Mycology 2011; 49: 561-80.

5. Ashbee HR, Barnes RA, Johnson EM, Richardson MD, Gorton R, Hope WW. Therapeutic drug monitoring (TDM) of antifungal agents: guidelines from the British Society for Medical Mycology. The Journal of antimicrobial

chemotherapy 2014; 69: 1162-76.

6. Stott KE, Hope WW. Therapeutic drug monitoring for invasive mould infections and disease: pharmacokinetic and pharmacodynamic considerations. Journal of Antimicrobial Chemotherapy 2017; 72: i12-i18.

7. Theuretzbacher U, Ihle F, Derendorf H. Pharmacokinetic/pharmacodynamic profile of voriconazole. Clinical pharmacokinetics 2006; 45: 649-63.

8. Hyland R, Jones B, Smith D. Identification of the cytochrome P450 enzymes involved in the N-oxidation of voriconazole. Drug metabolism and disposition 2003; 31: 540-47.

9. Weiss J, Hoevel MM, Burhenne J, Walter-Sack I, Hoffmann MM, Rengelshausen J, Haefeli WE, Mikus G. CYP2C19 genotype is a major factor contributing to the highly variable pharmacokinetics of voriconazole. The Journal of Clinical Pharmacology 2009; 49: 196-204.

10. Lee S, Kim BH, Nam WS, Yoon SH, Cho JY, Shin SG, Jang IJ, Yu KS. Effect of CYP2C19 polymorphism on the

pharmacokinetics of voriconazole after single and multiple doses in healthy volunteers. Journal of clinical pharmacology 2012; 52: 195-203.

11. Owusu Obeng A, Egelund EF, Alsultan A, Peloquin CA, Johnson JA. CYP2C19 polymorphisms and therapeutic drug monitoring of voriconazole: are we ready for clinical implementation of pharmacogenomics? Pharmacotherapy 2014; 34: 703-18.

12. Chung H, Lee H, Han H, An H, Lim KS, Lee YJ, Cho J-Y, Yoon SH, Jang I-J, Yu K-S. A pharmacokinetic comparison of two voriconazole formulations and the effect of CYP2C19 polymorphism on their pharmacokinetic profiles. Drug design, development and therapy 2015; 9: 2609.

13. Han SM, Park J, Lee JH, Lee SS, Kim H, Han H, Kim Y, Yi S, Cho JY, Jang IJ, Lee MG. Targeted Next-Generation Sequencing for Comprehensive Genetic Profiling of Pharmacogenes. Clinical pharmacology and therapeutics 2017; 101: 396-405.

14. Namgoong S, Cheong HS, Kim JO, Kim LH, Na HS, Koh IS, Chung MW, Shin HD. Comparison of genetic variations of the SLCO1B1, SLCO1B3, and SLCO2B1 genes among five ethnic groups. Environmental Toxicology and Pharmacology 2015; 40: 692-97.

15. Gautier-Veyret E, Fonrose X, Tonini J, Thiebaut-Bertrand A, Bartoli M, Quesada JL, Bulabois CE, Cahn JY, Stanke-Labesque F. Variability of voriconazole plasma concentrations after allogeneic hematopoietic stem cell transplantation: impact of cytochrome p450 polymorphisms and comedications on initial and subsequent trough levels. Antimicrobial agents and chemotherapy 2015; 59: 2305-14.

16. Elens L, van Gelder T, Hesselink DA, Haufroid V, van Schaik RH. CYP3A4*22: promising newly identified CYP3A4 variant allele for personalizing pharmacotherapy. Pharmacogenomics 2013; 14: 47-62.

17. Watanabe M, Kumai T, Matsumoto N, Tanaka M, Suzuki S, Satoh T, Kobayashi S. Expression of CYP3A4

mRNA is correlated with CYP3A4 protein level and metabolic activity in human liver. Journal of pharmacological sciences 2004; 94: 459-62.

18. Takagi S, Nakajima M, Mohri T, Yokoi T. Post-transcriptional regulation of human pregnane X receptor by micro-RNA affects the expression of cytochrome P450 3A4. Journal of biological chemistry 2008; 283: 9674-80.

19. Ohtsuki S, Schaefer O, Kawakami H, Inoue T, Liehner S, Sato A, Ishiguro N, Kishimoto W, Ludwig-Schwellinger E, Ebner T. Simultaneous absolute protein quantification of transporters, cytochrome P450s and UDP-glucuronosyltransferases as a novel approach for the characterization of individual human liver: comparison with mRNA levels and activities. Drug metabolism and Disposition 2011: dmd. 111.042259.

20. Willrich MAV, Hirata MH, Hirata RDC. Statin regulation of CYP3A4 and CYP3A5 expression. Pharmacogenomics 2009; 10: 1017-24.

21. Temesvari M, Kobori L, Paulik J, Sárváry E, Belic A,

Monostory K. Estimation of drug–metabolizing capacity by cytochrome P450 genotyping and expression. Journal of Pharmacology and Experimental Therapeutics 2012; 341: 294–305.

22. Wei Z, Jiang S, Zhang Y, Wang X, Peng X, Meng C, Liu Y, Wang H, Guo L, Qin S. The effect of microRNAs in the regulation of human CYP3A4: a systematic study using a mathematical model. Scientific reports 2014; 4: 4283.

23. Shin KH, Choi M, Lim K, Yu KS, Jang IJ, Cho JY. Evaluation of endogenous metabolic markers of hepatic CYP3A activity using metabolic profiling and midazolam clearance. Clinical Pharmacology & Therapeutics 2013; 94: 601–09.

24. Lee J, Kim AH, Yi S, Lee S, Yoon SH, Yu K–S, Jang I–J, Cho J–Y. Distribution of exogenous and endogenous CYP3A markers and related factors in healthy males and females. The AAPS journal 2017; 19: 1196–204.

25. Shin K–H, Ahn LY, Choi MH, Moon J–Y, Lee J, Jang I–J, Yu K–S, Cho J–Y. Urinary 6β–

hydroxycortisol/cortisol ratio most highly correlates with midazolam clearance under hepatic CYP3A inhibition and induction in females: a pharmacometabolomics approach. The AAPS journal 2016; 18: 1254-61.

26. Yun Kim. A Population Pharmacokinetic Analysis of Voriconazole and Development of a Personalized CYP2C19 Genotype-Guided Voriconazole Dosing Regimen: Seoul National University, 2019.

27. Pascual A, Calandra T, Bolay S, Buclin T, Bille J, Marchetti O. Voriconazole therapeutic drug monitoring in patients with invasive mycoses improves efficacy and safety outcomes. Clinical infectious diseases 2008; 46: 201-11.

28. Owusu Obeng A, Egelund EF, Alsultan A, Peloquin CA, Johnson JA. CYP 2C19 Polymorphisms and Therapeutic Drug Monitoring of Voriconazole: Are We Ready for Clinical Implementation of Pharmacogenomics? Pharmacotherapy: The Journal of Human Pharmacology and Drug Therapy 2014; 34: 703-18.

29. Berge M, Guillemain R, Boussaud V, Pham MH, Chevalier P, Batisse A, Amrein C, Dannaoui E, Loriot MA, Lillo-Le Louet A, Billaud EM. Voriconazole pharmacokinetic variability in cystic fibrosis lung transplant patients. Transplant infectious disease : an official journal of the Transplantation Society 2009; 11: 211-9.

30. Dolton MJ, Mikus G, Weiss J, Ray JE, McLachlan AJ. Understanding variability with voriconazole using a population pharmacokinetic approach: implications for optimal dosing. Journal of Antimicrobial Chemotherapy 2014; 69: 1633-41.

31. Kalliokoski A, Niemi M. Impact of OATP transporters on pharmacokinetics. British journal of pharmacology 2009; 158: 693-705.

32. Knauer MJ, Urquhart BL, Meyer zu Schwabedissen HE, Schwarz UI, Lemke CJ, Leake BF, Kim RB, Tirona RG. Human skeletal muscle drug transporters determine local exposure and toxicity of statins. Circulation research 2010; 106: 297-306.

33. Johnson M, Patel D, Matheny C, Ho M, Chen L, Ellens H. Inhibition of Intestinal OATP2B1 by the Calcium Receptor Antagonist Ronacaleret Results in a Significant Drug-Drug Interaction by Causing a 2-Fold Decrease in Exposure of Rosuvastatin. Drug metabolism and disposition: the biological fate of chemicals 2017; 45: 27-34.

34. Mougey EB, Feng H, Castro M, Irvin CG, Lima JJ. Absorption of montelukast is transporter mediated: a common variant of OATP2B1 is associated with reduced plasma concentrations and poor response. Pharmacogenetics and genomics 2009; 19: 129-38.

35. Imanaga J, Kotegawa T, Imai H, Tsutsumi K, Yoshizato T, Ohyama T, Shirasaka Y, Tamai I, Tateishi T, Ohashi K. The effects of the SLCO2B1 c.1457C > T polymorphism and apple juice on the pharmacokinetics of fexofenadine and midazolam in humans. Pharmacogenetics and genomics 2011; 21: 84-93.

36. Lamba JK, Lin YS, Schuetz EG, Thummel KE. Genetic contribution to variable human CYP3A-mediated

metabolism. Advanced drug delivery reviews 2002; 54: 1271-94.

37. Paine, Mary F., et al. "The human intestinal cytochrome P450 “pie”." Drug Metabolism and Disposition 34.5 (2006): 880-886.

38. Zane, Nicole R., and Dhiren R. Thakker. "A physiologically based pharmacokinetic model for voriconazole disposition predicts intestinal first-pass metabolism in children." Clinical pharmacokinetics 53.12 (2014): 1171-1182.

39. Friberg, Lena E., et al. "Integrated population pharmacokinetic analysis of voriconazole in children, adolescents, and adults." Antimicrobial agents and chemotherapy 56.6 (2012): 3032-3042.

APPENDICES

1. R script for goodness of fit (GOF) plots

```
if(Sys.getenv("R_LIB") != "") { .libPaths(c(Sys.getenv("R_LIB"), .libPaths())) }

library(lattice)
library(grid)

req.fields <- c("DV", "PRED", "IPRED", "TIME", "CWRES")
models <- list (
  "run1045" = list (
    modelfile          = "run1045.ctl",
    description        = "RE_SLCO~all",
    reference_model = "run1027",
    working_dir        = "C:/NM/phd/run",
    data_file          = "..//PopPK_phd_2.csv",
    output_file        = "run1045.lst",
    tables             = c("sdtab1045","patab1045","cotab1045","catab1045"),
    estim              = list(
      th             = c(3.02E+01, 5.01E+01, 5.76E+01, 1.61E+01, 2.54E+01, 5.46E+01, 1.17E+00, 8.72E-01,
2.36E-01, 1.62E-01, 1.00E-02, 2.00E-03, 1.00E-04, 2.25E-01, 2.20E+00, 5.95E-01, -1.86E-01, -7.46E-01,
-5.10E-01, -4.40E-01, 2.56E+00, 1.00E-04, 7.99E-01, -7.50E-01),
```

```
      th_se         = c(5.97E+00, 1.86E+00, 4.48E+00, 2.02E+00, NA, NA, 3.81E-01, 3.38E-02, 4.48E-03, NA,
NA, NA, NA, 1.85E-02, NA, NA, NA, NA, NA, NA, NA, NA, NA, NA),
      om            = c(0.16, 0.014, 0, 0, 0.825, 0.526, 0, 0.259),
      om_se         = c(0.132,0.00466,0,0,0.434,0.391,0,0),
      om_block      = matrix(c( 0.16, -0.0212, 0, 0, 0, 0, 0, 0,
                               -0.0212, 0.014, 0, 0, 0, 0, 0, 0,
                                0, 0, 0, 0, 0, 0, 0, 0,
                                0, 0, 0, 0, 0, 0, 0, 0,
                                0, 0, 0, 0, 0.825, 0, 0, 0,
                                0, 0, 0, 0, 0, 0.526, 0, 0,
                                0, 0, 0, 0, 0, 0, 0, 0,
                                0, 0, 0, 0, 0, 0, 0, 0.259), ncol=8),
      om_se         = c(0.132,0.00466,0,0,0.434,0.391,0,0),
      si            = c( 1),
      si_se         = c(0),
      si_block      = matrix(c(1), ncol=1),
      si_se_block = matrix(c(0), ncol=1)
    )
  )
)
run_from <- list(software = "pirana", version = "2.9.7")
open_res <- 1

setwd('C:/NM/phd/run')
```

```
model_names <- names(models)
if (!file.exists("pirana_reports")) {dir.create ("pirana_reports")}
for (i in 1:length(model_names)) {
    fname <- paste("pirana_reports/",names(models)[i],"_GOF.pdf", sep="")
    header<- paste("Goodness of fit model",names(models)[i], sep=" ")
    if (file.exists (fname)){
        file.remove (fname)
    }
    mod       <- models[[model_names[i]]]
    tab_file <- c(mod$tables[grep("sdtab", mod$tables)])[1]
    if (is.na(tab_file)) { # then assume the first table has the gof variables
        tab_file <- mod$tables[1]
    }
    if (file.exists (tab_file)) {
        tab <- read.table (tab_file, skip=1, header=T) # NONMEM table with ONEHEADER option
        m <- match (names(models[[model_names[i]]]$input_trans), colnames(tab))          # tranlation of $INPUT
variables
        colnames(tab)[m] <- unlist (models[[model_names[i]]]$input_trans, use.names=F) # tranlation of $INPUT
variables
        if ("MDV" %in% names(tab)) { tab <- tab[tab$MDV==0,] }                          # check if MDV present
        if ("EVID" %in% names(tab)) { tab <- tab[tab$EVID==0,] }                        # check if EVID present
        not.found <- req.fields[is.na(match(req.fields, colnames(tab)))]
        if ( length (not.found) > 0) {
          cat (paste("The variable(s)",not.found,"were not found. Please check your output tables.\nStopping R
```

```
execution."))
          quit()
        }
#####################################################################
# R code for plotting starts here
        pan2 <- function(x,y,...)      {
             panel.xyplot(x,y,...)
             panel.abline(0,1,col="black")
             panel.loess(x,y,col="red", lwd=1)
             }

        pan3 <- function(x,y,...)      {
             panel.xyplot(x,y,...)
             panel.abline(0,0,col="black")
             panel.abline(1.96,0,col="black",lty=2)
             panel.abline(-1.96,0,col="black",lty=2)
             panel.lmline(x,y,col="red",lwt=2)
        }

        ipredlim       <- range(tab$IPRED) * c(0.95, 1.05)
        dvlim          <- range(tab$DV) * c(0.95, 1.05)
        lim1           <- range(c(ipredlim, dvlim))
        reslim         <- range(tab$CWRES) * 1.05
        tick <- c(-5,-2,0,2,5)
```

```
pl1 <-          xyplot(DV~IPRED, data=tab,
                 panel=pan2,
                 type="p", cex=0.5,
                 ylab=list("Observed concentration",cex=0.7, just=c(0.5,2.5)),
                 xlab=list("Individual predicated concentration", cex=0.7, just=c(0.5,-1)),
                 scales=list (tck=c(1, 0),x=list(cex=0.5),y= list(cex=0.5)),
                 ylim=lim1,
                 xlim=lim1,
                 main=list("Individual predictions versus concentrations",cex=0.55,just=c(0.43,4))
                 )

pl2 <-          xyplot(DV~PRED, data=tab,
                 panel=pan2,
                 type="p", cex=0.5,
                 ylab=list("Observed concentration",cex=0.7, just=c(0.5,2.5)),
                 xlab=list("Population predicated concentration",cex=0.7,just=c(0.5,-1)),
                 ylim=lim1,
                 xlim=lim1,
                 scales=list (tck=c(1, 0),x=list(cex=0.5),y= list(cex=0.5)),
                 main=list("Population predictions versus concentrations",cex=0.55,just=c(0.43,4))
                 )

pl3 <-          xyplot(CWRES~PRED, data=tab,
```

```
                        ylim=reslim,
                        panel=pan3,
                        type="p", cex=0.5,
                        ylab=list("CWRES",cex=0.5, just=c(0.7,3)),
                        xlab=list(" Population predicted concentration", cex=0.7,just=c(0.5,-1)),
                        scales=list (tck=c(1, 0),x=list(cex=0.5),y= list(cex=0.5, at=tick)),
                        main=list("Conditional weighted residuals versus population
predictions",cex=0.55,just=c(0.43,4))
                        )

        pl4 <-          xyplot(CWRES~TAD, data=tab,
                        ylim=reslim,
                        panel=pan3,
                        type="p", cex=0.5,
                        ylab=list("CWRES",cex=0.5, just=c(0.7,3)),
                        xlab=list(" Time after dose", cex=0.7,just=c(0.5,-1)),
                        scales=list (tck=c(1, 0),x=list(cex=0.5),y= list(cex=0.5, at=tick)),
                        main=list("Conditional weighted residuals versus time",cex=0.55,just=c(0.43,4))
                        )

##########################################################################
    } else {
        cat (paste("The table file ",tab_file," was not found. Please check your output tables.\nStopping R execution."))
        quit()
```

```
    }
    pdf (file = fname)
    print(pl3, position=c(0,-0.01,      0.52,0.51)   , more=TRUE)
    print(pl4, position=c(0.48,-0.01, 1,0.51)        , more=TRUE)
    print(pl1, position=c(0,0.45,       0.52,0.99)   , more=TRUE)
    print(pl2, position=c(0.48,0.45,   1,0.99)       , more=TRUE)
    grid.text(header,y = 0.98)
    dev.off()

    # open created file
    cat (paste("OUTPUT: ", fname, sep=""))
    if (file.exists(fname) && open_res) {
        if (Sys.info()['sysname'] == 'Windows') { shell.exec(paste(getwd(),"/",fname,sep="")) }   # windows
       else if (Sys.info()['sysname'] == 'Darwin') { system(paste ("open ",fname, sep="")) } # mac
      else { system(paste("xdg-open ", fname, sep=""), ignore.stdout=TRUE, ignore.stderr=TRUE, wait=FALSE) }
# linux
    }
}

quit()
```

2. R script for visual predictive check (VPC)

```
if(Sys.getenv("R_LIB") != "") { .libPaths(c(Sys.getenv("R_LIB"), .libPaths())) }

library(xpose4)
library(ggplot2)
library(reshape)

models <- list (
  "run1045" = list (
    modelfile          = "run1045.ctl",
    description        = "RE_SLCO~all",
    reference_model = "run1027",
    working_dir        = "C:/NM/phd/run",
    data_file          = "..//PopPK_phd_2.csv",
    output_file        = "run1045.lst",
    tables             = c("sdtab1045","patab1045","cotab1045","catab1045"),
    estim              = list(
      th             = c(3.02E+01, 5.01E+01, 5.76E+01, 1.61E+01, 2.54E+01, 5.46E+01, 1.17E+00, 8.72E-01,
2.36E-01, 1.62E-01, 1.00E-02, 2.00E-03, 1.00E-04, 2.25E-01, 2.20E+00, 5.95E-01, -1.86E-01, -7.46E-01,
-5.10E-01, -4.40E-01, 2.56E+00, 1.00E-04, 7.99E-01, -7.50E-01),
      th_se          = c(5.97E+00, 1.86E+00, 4.48E+00, 2.02E+00, NA, NA, 3.81E-01, 3.38E-02, 4.48E-03, NA,
NA, NA, NA, 1.85E-02, NA, NA, NA, NA, NA, NA, NA, NA, NA, NA),
      om             = c(0.16, 0.014, 0, 0, 0.825, 0.526, 0, 0.259),
```

```
      om_se         = c(0.132,0.00466,0,0,0.434,0.391,0,0),
      om_block      = matrix(c( 0.16, -0.0212, 0, 0, 0, 0, 0, 0,
                               -0.0212, 0.014, 0, 0, 0, 0, 0, 0,
                                0, 0, 0, 0, 0, 0, 0, 0,
                                0, 0, 0, 0, 0, 0, 0, 0,
                                0, 0, 0, 0, 0.825, 0, 0, 0,
                                0, 0, 0, 0, 0, 0.526, 0, 0,
                                0, 0, 0, 0, 0, 0, 0, 0,
                                0, 0, 0, 0, 0, 0, 0, 0.259), ncol=8),
      om_se         = c(0.132,0.00466,0,0,0.434,0.391,0,0),
      si            = c( 1),
      si_se         = c(0),
      si_block      = matrix(c(1), ncol=1),
      si_se_block = matrix(c(0), ncol=1)
    )
  )
)
run_from <- list(software = "pirana", version = "2.9.7")
open_res <- 1

setwd('C:/NM/phd/run')
folder <-   "vpc_run1045"

command <- readLines(paste(folder, "/command.txt", sep=""))
```

```
args <- strsplit(command, " ")[[1]][-1]
for (i in seq(args)) { if(substr(args[i],0,1) != "-") { modfile <- args[i] } }
runno <- strsplit(modfile, "\\.")[[1]][1]

csv_file <- dir(folder, pattern="raw_result")[1]
fname <- paste("pirana_reports/vpc_", folder, ".pdf", sep="")
if (runno != "") {
  fname <- paste("pirana_reports/",runno,"_vpc_", folder, ".pdf", sep="")
}
if (!file.exists("pirana_reports")) {dir.create ("pirana_reports")}
if (file.exists (paste("pirana_reports/vpc_",folder,".pdf", sep=""))){
    file.remove (paste("pirana_reports/vpc_",folder,".pdf", sep=""))
}

vpc.info <- paste(folder,"/vpc_results.csv", sep="")
vpctab <- paste(folder, "/", dir(folder, pattern = "^vpctab")[1], sep="")
if (!file.exists(vpctab)|!(file.exists(vpc.info))) {
  cat ("VPC output not found. The vpc in PsN probably failed.")
  quit()
}
tab <- read.vpctab(vpctab)
vpc <- read.npc.vpc.results(vpc.info)
vpc_tmp <- data.frame(vpc$result.tables[-length(vpc$result.tables)])
tab_dat <- tab@Data
```

```
## handle stratification (if present)
strat_id <- grep("lower", names(vpc_tmp))
if (length(strat_id) > 1) {
  strat_id <- c(grep("lower", names(vpc_tmp)), (length(vpc_tmp[1,])+1))
  vpc_dat <- c()
  for (i in 1:(length(strat_id)-1)) {
    tmp <- cbind(vpc_tmp[,c(strat_id[i]:(strat_id[i+1]-1))], strata_no = i)
    if (i>1) { colnames(tmp) <- colnames(vpc_dat) }
    vpc_dat <- rbind(vpc_dat, tmp)
  }
  vpc_dat$strata_name <- vpc$strata.names[vpc_dat$strata_no]
  tab_dat$strata_name <- vpc$strata.names[tab_dat$strata]
  pl <- ggplot (tab_dat, aes(group=factor(as.character(strata_name)))) + facet_wrap ( ~ strata_name)
} else {
  vpc_dat <- vpc_tmp
  pl <- ggplot (tab_dat)
}

# enlarge limits to allow plotting of confidence intervals
xlim <- c(min(c(vpc_dat$lower, tab_dat$TIME), na.rm=TRUE), max(c(vpc_dat$upper, tab_dat$TIME),
na.rm=TRUE))
ylim <- c(min(c(vpc_dat[["X95.CI.for.5.from"]], tab_dat$DV), na.rm=TRUE), max(c(vpc_dat[["X95.CI.for.95.to"]],
tab_dat$DV), na.rm=TRUE))
```

```
# for unbinned VPCs
if (is.na(vpc_dat$lower[1])) {
  vpc_dat$lower <- vpc_dat$upper - min(diff(vpc_dat$upper))/2
  vpc_dat$upper <- vpc_dat$upper + min(diff(vpc_dat$upper))/2
  xlim[2] <- xlim[2] *1.02
}

# plot all layers
pl <- pl +
    geom_ribbon(data=vpc_dat, aes(x=(upper+lower)/2, ymin=vpc_dat[["X95.CI.for.5.from"]],
ymax=vpc_dat[["X95.CI.for.5.to"]]), linetype=0, alpha=0.2, fill="#002288") +
    geom_ribbon(data=vpc_dat, aes(x=(upper+lower)/2, ymin=vpc_dat[["X95.CI.for.95.from"]],
ymax=vpc_dat[["X95.CI.for.95.to"]]), linetype=0, alpha=0.2, fill="#002288") +
    geom_ribbon(data=vpc_dat, aes(x=(upper+lower)/2, ymin=vpc_dat[["X95.CI.for.50.from"]],
ymax=vpc_dat[["X95.CI.for.50.to"]]), linetype=0, alpha=0.2, fill="#882222") +
    geom_point(data=tab_dat, aes(TAD, DV), colour="#444444") +
    geom_line(data=vpc_dat, aes( (vpc_dat$upper+vpc_dat$lower)/2, vpc_dat[["X50.real"]]), size=1.5,
colour="#882222") +
    geom_line(data=vpc_dat, aes( (vpc_dat$upper+vpc_dat$lower)/2, vpc_dat[["X5.real"]]), size=.5,
linetype="solid", colour="#222288") +
    geom_line(data=vpc_dat, aes( (vpc_dat$upper+vpc_dat$lower)/2, vpc_dat[["X95.real"]]), size=.5,
linetype="solid", colour="#222288") +
    xlab ("Time after dose (hr)") +
```

```
    ylab ("Dependent variable") +
    xlim (xlim) +
    ylim (ylim)

pdf(file=fname, height=6, width=8)
print (pl)
dev.off()

## open created file
cat (paste("OUTPUT: ", fname, sep=""))
if (file.exists(fname) && open_res) {
    if (Sys.info()['sysname'] == 'Windows') { shell.exec(paste(getwd(),"/",fname,sep="")) }   # windows
    else if (Sys.info()['sysname'] == 'Darwin') { system(paste ("open ",fname, sep="")) } # mac
    else { system(paste("xdg-open ", fname, sep=""), ignore.stdout=TRUE, ignore.stderr=TRUE, wait=FALSE) }
# linux
}

quit()
```

국문 초록

서론: Voriconazole 의 높은 약동학적 변동성은 주로 CYP2C19 의 유전형에 의해 설명할 수 있지만, 아직 변동성에 기여하는 인자 중 밝혀지지 않은 것들이 많다.

방법: 본 연구에서는 solute carrier organic anion transporter family member 2B1 (SLCO2B1)의 유전형이 voriconazole 의 약동학에 미치는 영향을 탐색하고자 12 명의 건강한 CYP2C19 poor metabolizer 를 대상으로 voriconazole 200 mg 을 단회 정맥 또는 경구 투여하였다. 모델 기반 시뮬레이션을 통해 voriconazole 반복 투여 시 SLCO2B1 유전형이 약동학에 미치는 영향을 탐색하였다. 추가로, CYP3A4 효소의 활성도가 voriconazole 의 약동학에 미치는 영향도 탐색하였다.

결과: Voriconazole 경구 투여 시 SLCO2B1 c.*396T>C variant type 대상자들은 wild type 대상자들에 비해 voriconazole의 흡수가 감소하는 양상이 관찰되었다. 하지만, 본 연구에서 측정된 CYP3A 활성도 표지자들은 voriconazole의 대사와 유의한 상관관계를 보이지 못했다. 모델 기반 시뮬레이션 결과, SLCO2B1 유전형은 voriconazole 표준 용법 반복 투여 시 치료적 범위에 도달하는 확률에 유의한 영향을 미치지 않았다.

결론: 본 연구의 결과는 SLCO2B1 c.*396T>C 이 장내 OATP2B1 의 기능 저하와 연관되었을 가능성과 voriconazole 의 개인간 약동학적 변이에 기여할 수 있음을 시사한다. 추가적인 연구를 통해 이러한 결과의 임상적 유의성을 확인할 필요가 있다.

* 본 내용의 일부는 *the Pharmacogenomics Journal* 학술지 (LEE, Sang Won, et al. *The Pharmacogenomics Journal*, 2020, 1-9; https://doi.org/10.1038/s41397-020-0166-1)에 출판 완료 된 내용임.

주요어 : 보리코나졸, 약물 수송체, SLCO2B1, 약동학, 약물유전체학

학 번 : 2014-22029